The Company of **Biologists**

RESEARCH ARTICLE

AP-1 family members act with Sox9 to promote chondrocyte hypertrophy

Xinjun He[1],*, Shinsuke Ohba[2],*, Hironori Hojo[1] and Andrew P. McMahon[1],‡

ABSTRACT

An analysis of Sox9 binding profiles in developing chondrocytes identified marked enrichment of an AP-1-like motif. Here, we have explored the functional interplay between Sox9 and AP-1 in mammalian chondrocyte development. Among AP-1 family members, *Jun* and *Fosl2* were highly expressed within prehypertrophic and early hypertrophic chondrocytes. Chromatin immunoprecipitation followed by DNA sequencing (ChIP-seq) showed a striking overlap in Jun- and Sox9-bound regions throughout the chondrocyte genome, reflecting direct binding of each factor to the same enhancers and a potential for protein-protein interactions within AP-1- and Sox9-containing complexes. *In vitro* reporter analysis indicated that direct co-binding of Sox9 and AP-1 at target motifs promoted gene activity. By contrast, where only one factor can engage its DNA target, the presence of the other factor suppresses target activation consistent with protein-protein interactions attenuating transcription. Analysis of prehypertrophic chondrocyte removal of *Sox9* confirmed the requirement of *Sox9* for hypertrophic chondrocyte development, and *in vitro* and *ex vivo* analyses showed that AP-1 promotes chondrocyte hypertrophy. Sox9 and Jun co-bound and co-activated a *Col10a1* enhancer in Sox9 and AP-1 motif-dependent manners consistent with their combined action promoting hypertrophic gene expression. Together, the data support a model in which AP-1 family members contribute to Sox9 action in the transition of chondrocytes to the hypertrophic program.

KEY WORDS: Chondrocyte development, Hypertrophy, Sox9, Transcriptional program, Mouse

INTRODUCTION

The SRY-box (Sox) transcriptional regulator Sox9 is a central regulator of endochondral skeletal development (reviewed by Akiyama and Lefebvre, 2011; Lefebvre and Dvir-Ginzberg, 2016). Initial *Sox9* expression in condensing mesenchymal cells precedes active chondrogenesis (Bi et al., 1999). Subsequently, *Sox9* expression is maintained in proliferating immature chondrocytes and post-mitotic prehypertrophic chondrocytes (Akiyama et al., 2005; Dy et al., 2012). *Sox9* transcription terminates in early hypertrophic chondrocytes (Dy et al., 2012). However, Sox9 protein persists through hypertrophic development:

[1]Department of Stem Cell Biology and Regenerative Medicine, Eli and Edythe Broad CIRM Center for Regenerative Medicine and Stem Cell Research, W.M. Keck School of Medicine, University of Southern California, Los Angeles, CA 90033, USA. [2]Department of Bioengineering, the University of Tokyo, Tokyo 113-0033, Japan.
*These authors contributed equally to this work

‡Author for correspondence (amcmahon@med.usc.edu)

A.P.M., 0000-0002-3779-1729

only terminal hypertrophic chondrocytes at the hypertrophic-osteoblast interface of the bone shaft lack Sox9 (Dy et al., 2012).

Genetic analysis in the mouse has shown that *Sox9* is necessary for establishing chondrocytes in the cranial, axial and appendicular skeleton (Akiyama et al., 2002; Bi et al., 2001; Mori-Akiyama et al., 2003). Moreover, Sox9 is sufficient to initiate chondrogenic programs when activated in mesenchymal stem cells (Ikeda et al., 2004), embryonic stem cells (Ikeda et al., 2004) and human dermal fibroblasts (Ikeda et al., 2004; Ohba et al., 2015; Outani et al., 2013). Inactivating mutations in human *SOX9* result in campomelic dysplasia, an autosomal dominant disorder characterized by hypoplasia of the endochondral skeleton and bowing of skeletal elements (Foster, 1996; Giordano et al., 2001; Kwok et al., 1995). Molecular studies indicate that Sox9 promotes expression of a broad spectrum of cartilage matrix components, promotes cell division and cell survival, and inhibits chondrocytes from adopting an alternative pathway of osteoblast development (reviewed by Lefebvre and Dvir-Ginzberg, 2016).

Sox9 directs chondrogenic programs in concert with other transcriptional components, notably the related Sox members Sox5 and Sox6. The combinatorial interaction of Sox5, Sox6 and Sox9 at *Acan* and *Col2a1* enhancers promotes the expression of these key genes within mitotic chondrocytes (reviewed by Akiyama and Lefebvre, 2011; Lefebvre, 2002). Although genome-wide binding analysis of Sox9 and Sox6 indicates that they co-regulate genomic targets within proliferating chondrocytes (Liu and Lefebvre, 2015), Sox action in hypertrophic chondrocyte development is less clear.

Genetic removal of *Sox9* broadly within both proliferating and prehypertrophic chondrocytes prevents hypertrophic progression. In the absence of Sox9, chondrocytes switch fate generating ectopic osteoblasts (Dy et al., 2012). *Runx2*, a key transcriptional regulator promoting hypertrophic chondrocyte development, is expressed in mitotic and postmitotic chondrocytes of the growth plate where Runx2 has been proposed to counter Sox9's transactivation of early chondrocyte targets such as *Col2a1* (Cheng and Genever, 2010; Zhou et al., 2006). Sox9 has also been reported to interact with Mef2 to activate *Col10a1*, a matrix-encoding gene specifically expressed by hypertrophic chondrocytes (Dy et al., 2012). Furthermore, other reports suggest that a Gli-Sox9 interaction at a distal enhancer of *Col10a1* suppresses *Col10a1* expression in proliferating chondrocytes (Leung et al., 2011). Together, these studies suggest that Sox9 actions on chondrocyte programs are temporally and spatially regulated by interplay with a variety of additional transcriptional regulators.

Direct analysis of DNA binding has been particularly insightful in distinguishing conflicting regulatory models. Recently, we performed a genome-scale analysis comparing Sox9-DNA interactions in somite-derived and neural crest-derived chondrocytes (Ohba et al., 2015). Analysis of motif recovery identified a highly significant enrichment of an activator protein-1 (AP-1) motif, suggesting co-integration of AP-1 factor engagement into a Sox9-driven

DEVELOPMENT

chondrocyte regulatory network. AP-1 family members have been linked to osteoblast and osteoclast regulation (reviewed by Wagner, 2002; Wagner and Eferl, 2005) and joint formation (Kan and Tabin, 2013) where Sox9 is either absent or present only at low levels. However, *Fosl2* mutants show a reduction in the hypertrophic chondrocyte zone and in mineralized hypertrophic cartilage matrix (Karreth et al., 2004) whereas *Jun* removal delays chondrocyte hypertrophy specifically in the baso-occipital bone (Behrens et al., 2003).

Here, we explored Sox9, Jun and Fosl2 interactions in the developing mouse skeleton. *Jun* and *Fosl2* are specifically expressed in prehypertrophic and early hypertrophic chondrocytes where endogenous *Sox9* levels are maximal. ChIP-seq analysis shows extensive overlap between Jun- and Sox9-bound genomic target regions in mouse primary rib chondrocytes. DNA association likely reflects both direct Jun DNA binding through AP-1 motifs, and indirect protein-protein association with Sox9 mediated by the DNA-binding region of Jun. *In vivo* and *in vitro* functional assays suggest that AP-1 and Sox9 co-regulatory pathways promote the chondrocyte transition to post-mitotic hypertrophic chondrocytes and activation of the hypertrophic chondrocyte marker gene *Col10a1*. These findings highlight the cooperative interplay of transcriptional programs underpinning development of the mammalian skeleton.

RESULTS

Jun and Fosl2 are specifically expressed in prehypertrophic chondrocytes

Our recent ChIP-seq analysis of Sox9 action in mammalian chondrocytes identified a striking enrichment of an AP-1 factor binding motif (TGAG/CTCA), in addition to the expected Sox9 dimer and monomer motifs (Ohba et al., 2015), suggesting that AP-1 family members might act in conjunction with Sox9 to regulate the chondrogenic program.

To address potential AP-1 action, we performed RNA-seq on neonatal rib cartilage to examine the expression of all AP-1 family members that are known to interact with the recovered AP-1 motif: Jun (previously known as c-Jun), Junb, Jund, Fos (cFos), Fosb, Fosl1 (Fra1) and Fosl2 (Fra2). Several members of the AP-1 family showed significant rib chondrocyte expression through this analysis (Table S1). Given that AP-1 factors interchangeably form functional homodimer and heterodimer protein complexes (reviewed by Eferl and Wagner, 2003), the data raised the possibility of considerable heterogeneity in endogenous AP-1 complexes. Among the expressed family members, *Jun* and *Fosl2* show strong expression within hypertrophic chondrocytes (see below) and both are linked to chondrocyte development (Behrens et al., 2003; Hess et al., 2003; Kan and Tabin, 2013; Karreth et al., 2004); these two AP-1 family members were selected for further study.

In situ hybridization to limb and rib skeletal elements with *Jun* and *Fosl2* probes showed strong specific expression of both factors within prehypertrophic and early stage hypertrophic chondrocytes where *Col10a1* is first activated (Fig. 1A-D′; Fig. S1A). Immunostaining showed high levels of Jun and Sox9 within Ki67⁻Sp7⁺ prehypertrophic chondrocytes extending into the initial domain of Col10a1⁺ hypertrophic chondrocytes (Fig. 1E-I′; Fig. S1B). These data suggest a potential interplay between Sox9 and AP-1 members at this key transition point in cartilage development.

Co-occupancy of the chondrocyte genome by Sox9 and Jun

To address directly AP-1 action within this chondrocyte population, we performed ChIP-seq with anti-Jun antibody on rib chromatin
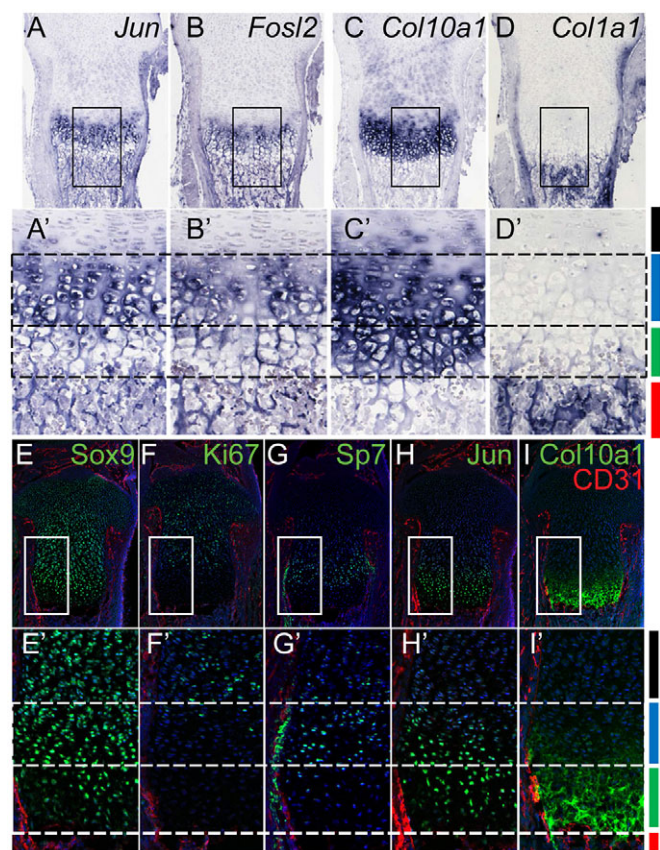

Fig. 1. *Jun* and *Fosl2* are specifically expressed in prehypertrophic and early hypertrophic chondrocytes. (A-D′) *In situ* hybridization comparing expression of *Jun*, *Fosl2*, *Col10a1* and *Col1a1* in the growth plate of the P1 mouse tibia. Boxed regions are magnified in A′-D′. (E-I′) Immunostaining of E17.5 mouse tibia sections to detect Sox9 (E), Jun (H), the proliferative cell marker Ki67 (F), the prehypertrophic chondrocyte marker Sp7 (G) and the hypertrophic chondrocyte marker Col10a1 (I). CD31 (red) demarcates the vasculature, and nuclei are visualized by DAPI staining (blue). Boxed regions appear as higher magnification images in E′-I′. Color bars on the right of D′ and I′ indicate distinct skeletal zones: red, bone-forming ossification region; green, mature hypertrophic chondrocytes; blue, prehypertrophic chondrocytes; black, columnar chondrocytes.

preparations previously used to define Sox9 interactions *in vivo* (Ohba et al., 2015). The populations used in both this study and the previous one (Ohba et al., 2015) include proliferating and prehypertrophic chondrocytes, but not mature hypertrophic chondrocytes. A Cisgenome analysis (Ji et al., 2008; Jiang et al., 2010) of the ChIP-seq data predicted a large number of Jun interaction sites: 99,162 peaks were significantly enriched above the input control. Motif recovery by MEME-ChIP (Bailey et al., 2009) and Cisgenome predicted a significantly enriched AP-1 consensus binding motif within the dataset (Fig. 2A; Table S2). An AP-1 motif was centered within Jun ChIP-seq peaks (Fig. S2A) and was present within a large percentage of recovered peaks (67.6%: 66,986 of 99,162) consistent with direct engagement of AP-1 complexes containing a Jun component. In summary, the general features of the dataset point to a comprehensive, highly confident set of genomic interactions for Jun within developing chondrocytes.

Next, we investigated the overlap of Jun ChIP-seq peaks with Sox9 Class II ChIP-seq peaks identified in our previous study (Ohba et al., 2015). The Class II peaks represent direct Sox9-bound cis-regulatory modules closely linked to the activation of chondrocyte-specific gene regulatory programs (Ohba et al., 2015). Surprisingly,
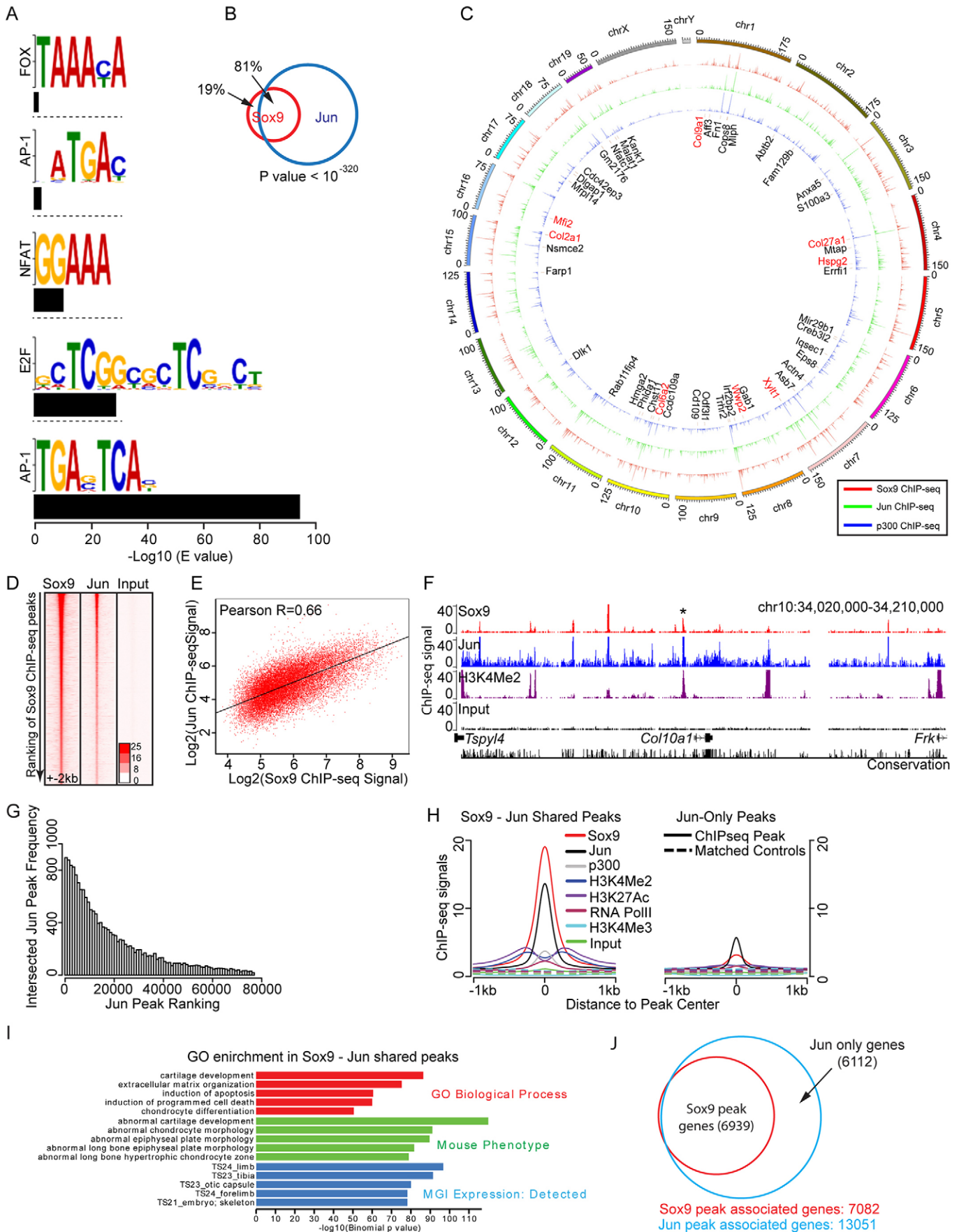
Fig. 2. See next page for legend.

Fig. 2. Co-occupation of Jun and Sox9 at putative cis-regulatory modules of chondrocyte target genes. (A) Motif recovery by MEME-ChIP program showing enriched motif logo within top 500 Jun ChIP-seq peaks. Black bars under each motif logo indicate significance of recovery expressed as −log10 of E value. (B) Venn diagram for Sox9 and Jun ChIP-seq peak intersection. The *P*-value indicates the significance in the overlap of Sox9 ChIP-seq peaks with Jun ChIP-seq peaks. (C) Circos correlation visualization of Sox9 and Jun ChIP-seq peaks. Individual Sox9, Jun and p300 ChIP-seq peaks were clustered based on their genomic coordinates onto reference mouse genome mm9. Clustered peaks were merged to show higher order clustering of ChIP-seq peaks. Super-enhancer associated genes are labeled (Ohba et al., 2015). Prominent extracellular matrix protein-encoding genes expressed in cartilage are highlighted in red. See also Fig. S3. (D) Heatmap of sequence reads at genomic loci around Sox9 ChIP-seq peaks. Signal intensity of Sox9 and Jun ChIP-seq were plotted ±2 kb from Sox9 ChIP-seq peak centers and ranked with Sox9 ChIP-seq peak ranking (Ohba et al., 2015). (E) Scatter plot of Sox9 and Jun ChIP-seq signal at Sox9 ChIP-seq peaks. *x*-axis and *y*-axis represent Sox9 and Jun ChIP-seq signals, respectively, at Sox9 ChIP-seq peaks. ChIP-seq signals are shown as log2 of sequence reads per peak per 10 million reads. (F) A screenshot of Sox9 Jun and H3K4Me2 ChIP-seq signal at *Col10a1* locus. Asterisk highlights the *Col10a1* hypertrophic enhancer module verified in published transgenic studies (Chambers et al., 2002; Gebhard et al., 2004; Leung et al., 2011; Li et al., 2011; Riemer et al., 2002; Zheng et al., 2009), which was explored in this study. (G) Intersection of Jun ChIP-seq peaks with Sox9 ChIP-seq peaks. *x*-axis indicates ranking of Jun ChIP-seq peaks determined by Cisgenome peak calling. *y*-axis indicates frequency of Jun ChIP-seq peaks intersected with Sox9 ChIP-seq peaks where each bin samples one hundred peaks. (H) Comparison of Sox9 and Jun ChIP-seq signals with ChIP-seq examining various histone modifications and general transcriptional components within Jun-Sox9 shared peak regions and Jun-only peak regions (±1 kb from peak center). Overlap of H3K4Me2, p300, H3K27Ac, RNAPolII demarcate active enhancer modules, whereas H3K4Me3 demarcates active promoters. Experimental samples were compared with matched controls to show specificity of the ChIP-seq signal. ChIP-seq signals are displayed as sequence reads per peak, per five nucleotides of every 10 million reads. (I) GREAT GO analysis of biological processes (red), mouse phenotype (green) and MGI expression (blue) in Jun-Sox9 shared peak regions. (J) Venn diagram of the intersection of nearest gene neighbors to Jun and Sox9 ChIP-seq peaks.

the majority of Sox9 Class II peaks (81%: 16,895 of 20,862) overlapped with Jun peaks (Fig. 2B); multiple interaction sites were prominent around genes encoding matrix proteins that are expressed at high levels in chondrocytes (Fig. 2C; Fig. S3). Furthermore, we observed a striking correlation in the relative levels of engagement between Jun and Sox9 at Jun-Sox9 co-bound regions (referred to as 'Jun-Sox9 shared peak regions' hereafter) as was reflected by the number of DNA sequence reads for bound regions (Fig. 2D,E). Importantly, Sox9 and Jun both associate strongly around *Col10a1*, a direct target of Sox9 regulation expressed in hypertrophic chondrocytes (Fig. 2F). Binding around *Col10a1* highlighted a previously identified hypertrophic DNA enhancer module 4 kb upstream of *Col10a1* that is sufficient to direct hypertrophic chondrocyte-restricted reporter gene expression *in vivo* (Fig. 2F) (Chambers et al., 2002; Gebhard et al., 2004; Leung et al., 2011; Li et al., 2011; Riemer et al., 2002; Zheng et al., 2009).

Interestingly, a comparison of DNA regions associated with Jun alone (referred to as 'Jun-only peak regions' hereafter) with those co-associated with Jun and Sox9 (Jun-Sox9 shared peaks) revealed several distinguishing features that suggest the latter are the most relevant to chondrocyte development. First, Jun-Sox9 shared peak regions showed a higher number of Jun sequence reads per peak and higher peak ranking consistent with stronger and/or more frequent engagement of Jun at sites co-engaged with Sox9 than Jun alone (Fig. 2G; Fig. S2B). Second, although both of these groups show strong enrichment of an AP-1 motif centered in peak regions indicative of *bona fide* Jun interactions with DNA targets

(Fig. S2A), a Sox9 motif is only enriched in Jun-Sox9 shared peak regions (Fig. S2A; Table S3). Furthermore, the strong centering of Jun and Sox9 motifs within ChIP-seq peaks suggests direct DNA engagement of both factors within some shared cis-regulatory elements but also the potential for indirect association through protein-protein interactions (see later). Third, comparison of Jun-binding data with our published analysis of active chondrocyte enhancer signatures (p300 binding, H3K4Me2 and H3K27 acetylation enrichment and RNA polymerase II engagement; Ohba et al., 2015) showed that active enhancer signatures predominated only within Jun-Sox9 shared peak regions (Fig. 2H). Together, these data lend additional weight to the biological relevance of the Jun and Sox9 component of the dataset in active transcriptional processes within chondrocytes. Fourth, the biological relevance of Jun-Sox9 shared peaks was underscored by GREAT gene ontology (GO) analysis associating bound regions with neighboring potential target genes (McLean et al., 2010). The Jun-Sox9 shared peak regions showed a highly significant association with skeletal GO terms; the top GO Biological Process term was 'cartilage development' and analysis of MGI expression terms predicted skeletal structures (Fig. 2I). Jun-only peaks also showed strong matrix organization GO term enrichment (Fig. S2C), suggesting that many of these identified weaker target sites around the same set of genes engaged by Sox9, a conclusion underscored by the observation that the predicted Sox9 target gene set is essentially entirely encompassed by the predicted Jun-target gene set (Fig. 2J). Given all the evidence here that Sox9 co-association identifies a chondrocyte-related Jun/AP-1 signature with the strongest feature of active enhancers, we focused our analysis on this component of the Jun dataset.

Jun and Sox9 interactions in the regulation of chondrocyte gene expression

To understand the molecular mechanisms underlying the interplay of Jun and Sox9 during chondrogenesis, we analyzed the distribution of AP-1 and Sox9 motifs in Jun-Sox9 shared peak regions. Compared with matched controls (position-matched random control regions bioinformatically calculated from the genome), we observed a strong, significant co-occurrence of Sox9 and AP-1 motifs: 39% in the whole dataset (Fig. 3A; *P*-value=1.8e-14) and 65% in the subset of peaks with a Sox9 dimer-binding motif (Fig. S4A; *P*-value<2.2e-16). Only 16% of predicted peaks failed to display a Sox9 or AP-1 binding site suggesting that direct DNA binding of Sox9, AP-1, or both factors, was the primary mode of Sox9 and Jun interaction at Jun-Sox9 shared peak regions (Fig. 3A). The Jun-Sox9 shared peak regions containing both Sox9 and AP-1 motifs showed a higher Sox9 ChIP-seq signal than those with only Sox9 motifs though each showed a comparable active enhancer signature (Fig. 3B; Fig. S4B). These data suggest an enhanced engagement of Sox9 when AP-1 was bound at adjacent DNA sites.

Although these results are consistent with cooperative binding interactions between Sox9 and AP-1 complexes at respective target sites, a significant number of the shared regions have only an AP-1 or Sox9 site suggesting protein-protein association between Sox9 and AP-1 complexes (Fig. 3A). Consistent with this view, Jun and Fosl2 co-immunoprecipitated with Sox9 when DNA-templated interactions were removed by digestion with the DNA nuclease benzonase (Fig. S4C). To further identify potential protein-protein interaction domains between Sox9 and Jun, we performed co-immunoprecipitation using a series of deletions directed by the domain architecture of each factor (Fig. 3C). These studies indicated that the N-terminal region of Sox9 interacts with a region of Jun
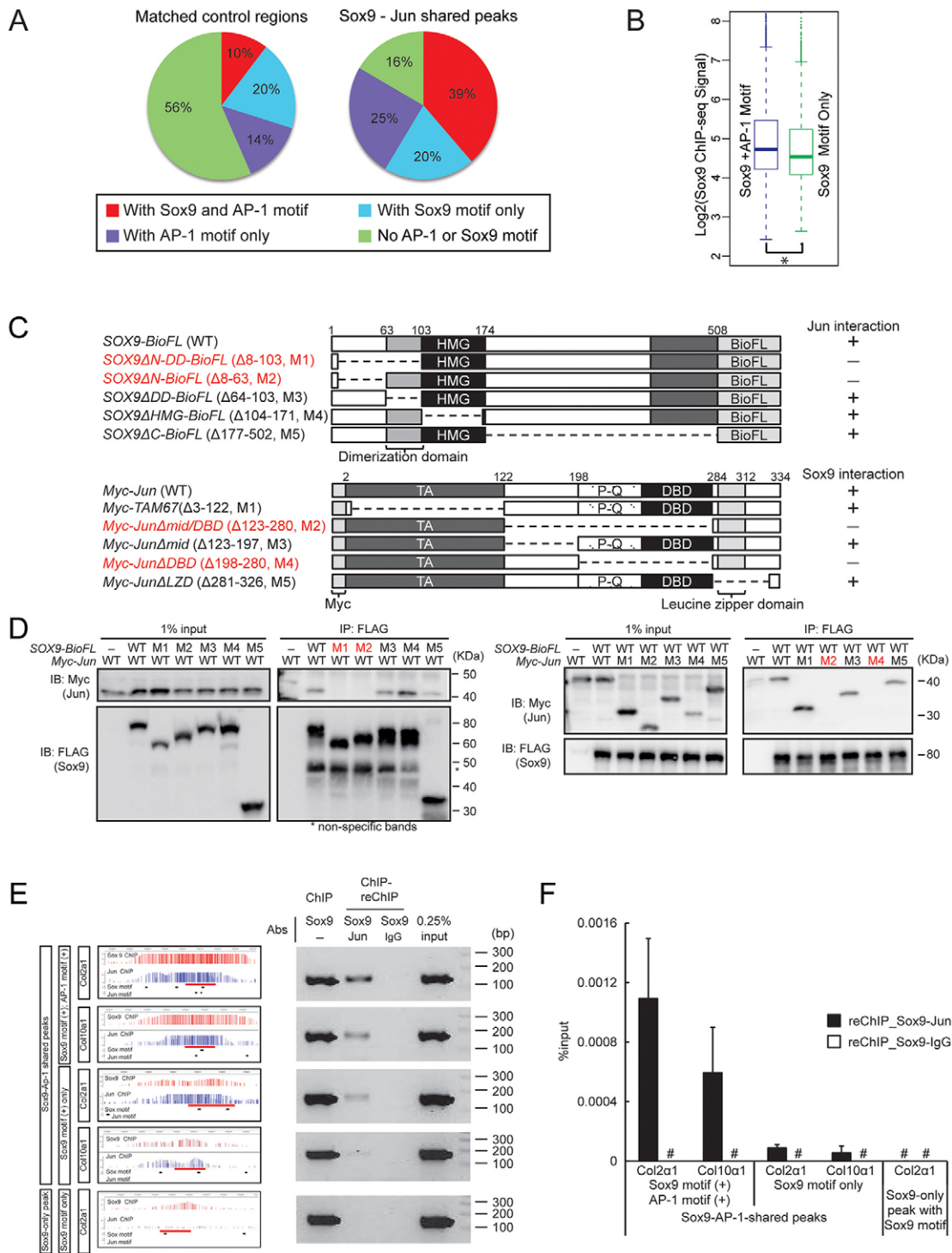
Fig. 3. Physical interaction between AP-1 factors and Sox9. (A) Enrichment of motifs in Jun-Sox9 shared peak regions. Compared with matched controls, Jun-Sox9 shared peak regions are categorized into four groups by the presence or absence of each factor's binding motif as indicated by the different colors. The pie charts show the frequency of each peak category. (B) Comparison of Sox9 ChIP-seq signal at Jun-Sox9 shared peak regions containing both Sox9 motif and AP-1 motifs (Sox9+AP-1 Motif) with those containing a Sox9 motif but no AP-1 motif (Sox9 Motif Only). *P=1.2e-13. (C) Diagram of deletion mutants used to determine Sox9 and Jun interactions (D). (D) Co-immunoprecipitation of Sox9 and Jun from HEK293T cells using serial deletion mutants illustrated in C. Deletions that prevent co-immunoprecipitation are highlighted in red. (E,F) Co-engagement of Sox9 and Jun on the chondrocyte genome. Following ChIP with the anti-Sox9 antibody, reChIP was performed as indicated. reChIP DNA was analyzed by conventional PCR (E) and quantitative PCR (F). Red bars in screenshots of CisGenome browser indicate regions analyzed by reChIP: (1) Sox9-AP-1-shared peaks with Sox9 and AP-1 motifs around the *Col2a1* gene (shared peak region, chr15:97856565-97857517; amplified region, chr15:97857031-97857184) and *Col10a1* gene (shared peak region, chr10:34076082-34076958; amplified region, chr10:34076498-34076672), (2) Sox9-AP-1-shared peaks only with Sox9 motif around the *Col2a1* gene (shared peak region, chr15:97855718-97856360; amplified region, chr15:97856092-97856262) and *Col10a1* gene (shared peak region, chr10:34062583-34063545; amplified region, chr10:34062970-34063158), and (3) Sox9-only peak with Sox9 motif around the *Col2a1* gene (peak region, chr15:97839111-97840087; amplified region, chr15:97839448-97839608). #, undetected. Error bars represent s.d.

encompassing the DNA-binding domain and adjacent proline/glutamine-enriched stretch (Fig. 3D).

We confirmed the protein-DNA-mediated and protein-protein-mediated interaction between Sox9 and AP-1 on the chondrocyte genome by ChIP-reChIP assay using the same chromatin preparations as those used in Sox9 and Jun ChIP-seq (Fig. 3E,F); enrichment was detected in (1) Sox9-AP-1-shared peaks with Sox9 and AP-1 motifs and (2) Sox9-AP-1-shared peaks with only Sox9 motif, but not in a Sox9-only peak with Sox9 motif, with more enrichment detected in (1) than in (2). These data, when considered with those in Fig. 3B and Fig. S4B, suggest that co-occupation of Sox9 and Jun within a cis-regulatory module may be promoted by the co-occurrence of each factor's recognition motif.

To understand the interplay of direct (protein-DNA mediated) and indirect (protein-protein mediated) Sox9 and AP-1 engagement on transcription of target genes, we generated a series of luciferase reporter constructs combining different enhancer-motif configurations with a basal promoter element: 4x48-Col2a1 (Fig. 4A; four copies of a 48 bp enhancer from *Col2a1* intron 1 that contains multiple Sox9 binding motifs but no AP-1 motifs; Kan et al., 2009); 3xSox9BS(Col9a1) (Fig. 4B; three copies of a 17-nucleotide Sox9 dimer-binding motif from the *Col9a1* enhancer; Ohba et al., 2015); 7xAP-1BS (Fig. 4C; seven copies of the optimal AP-1 motif); and 3xSox9BS(Col9a1)+7xAP-1BS (Fig. 4D; an artificial enhancer element combining Sox9 and AP-1 regulatory modules above).

As expected, Sox9 activated the 4x48-Col2a1 and 3xSox9BS (Col9a1) reporters (Fig. 4A,B). However, Sox9-mediated activation was reduced on co-transfection with Jun and Fosl2 (Fig. 4A,B). By contrast, TAM67, a dominant-negative variant of Jun that retains

DNA binding but has no transcriptional activation capability, specifically suppressed endogenous AP-1 function (Brown et al., 1993), but enhanced Sox9-mediated activation of the reporter, presumably reflecting TAM67 inhibition of endogenous AP-1 complexes (Fig. 4A,B; Fig. S4D). As expected, Jun alone, or together with Fosl2, promoted activity of the 7xAP-1BS reporter; however, their activity was suppressed by Sox9 (Fig. 4C). By contrast, maximal activation of the 3xSox9BS(Col9a1)+7xAP-1BS reporter required both Sox9 and AP-1 family members and reporter activity was reduced by co-transfection with TAM67 (Fig. 4D). Together, these data suggest that protein-protein association between Sox9 and AP-1 family members reduced the transactivation activity of either complex evident in the response of target enhancers where direct binding sites are only present for one Sox9 or AP-1 factor. However, an additive transcriptional activity occurs when the DNA target contains binding sites for both Sox9 and AP-1. Consequently, the overall effect of AP-1 members on Sox9 regulation of chondrocyte targets is likely to be complex, reflecting the distribution of each factor's direct binding sites within the regulatory genome and non-DNA-dependent co-interaction.

Sox9 and AP-1 positively regulate chondrocyte hypertrophy

To understand the functional significance of the interplay between Sox9 and AP-1 in chondrocyte differentiation, we utilized a drug, SR11302, that inhibits AP-1-mediated transcriptional activation (Fanjul et al., 1994). We confirmed first that SR11302 inhibited Jun-mediated activation of its target in a dose-dependent manner (Fig. S4E). Next, we analyzed the effects of SR11302 on the expression of a *Col10a1* enhancer-driven mCherry reporter (*Col10a1:mCherry*) (Maye et al., 2011) in primary mouse
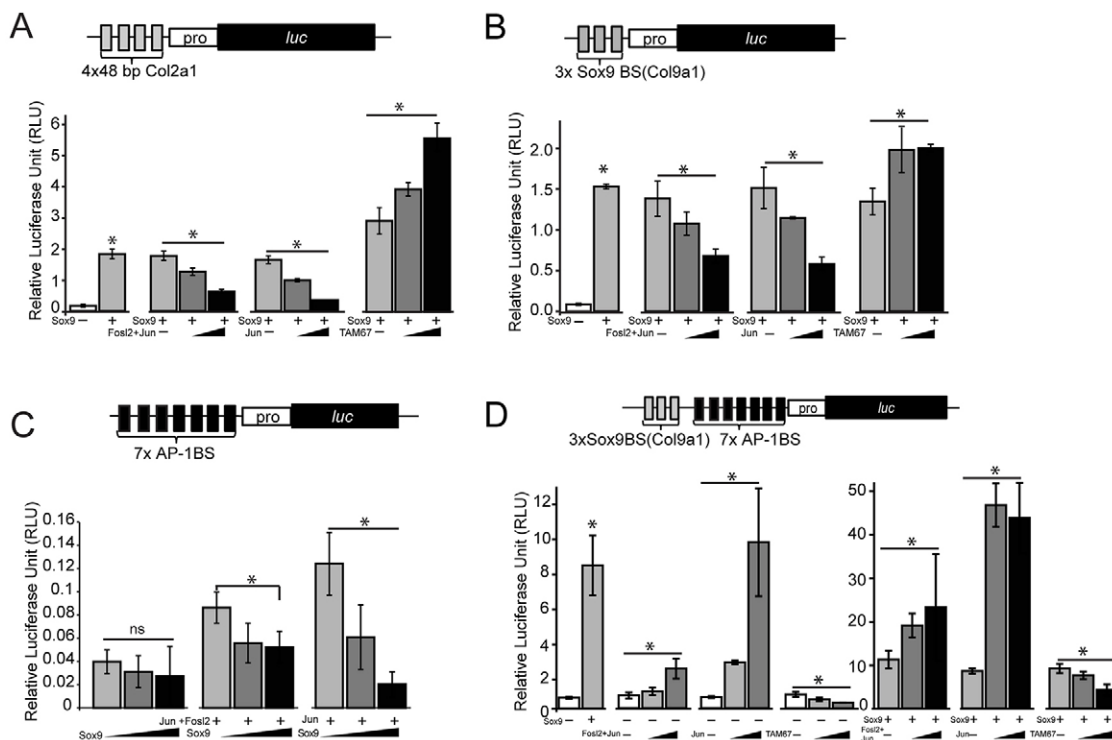

Fig. 4. Functional interactions between AP-1 factors and Sox9. (A-D) Reporter assay in HEK293T cells examining activation of a basal reporter luciferase construct containing four copies of a 48 bp *Col2a1* intron 1 enhancer module (4x48-Col2a1) (A), three copies of a 17-nucleotide sequence containing a Sox9-binding site in a *Col9a1* enhancer [3xSox9BS(Col9a1)] (B), seven copies of the AP-1 binding motif (7xAP-1BS) (C), and a module with both the 3xSox9BS (Col9a1) and 7xAP-1BS sequence (D). y-axis indicates relative light unit (RLU) values normalizing firefly luciferase to an internal *Renilla* luciferase control. *P <0.05; ns, non-significant. Error bars represent s.d.

transgenic chondrocytes. *Col10a1* is expressed in conjunction with *Jun* and *Fosl2* activation at the hypertrophic chondrocyte transition (Fig. 1). SR11302 downregulated *Col10a1:mCherry* reporter activity (Fig. 5A,B) and the endogenous levels of *Col10a1* mRNA (Fig. 5C). In addition, SR11302 inhibited normal activation of an endogenous *Col10a1:mCherry* transgenic reporter in intact femur explants, reducing the resulting hypertrophic zone and restricting ossification (Chung et al., 2001) (Fig. 5D). Whereas the levels of *Col2a1* (predominantly but not exclusively expressed in proliferating immature chondrocytes), *Sox9*, and a number of genes displaying similar expression levels within distinct chondrocyte cell types (*Actb*, *Epyc* and *Ndufv2*) were not significantly changed on SR11302 treatment, expression of prehypertrophic chondrocyte-enriched genes (*Sp7*, *Mef2c* and *Ihh*) was elevated (Fig. 5C; Fig. S4F). Collectively, these data support a model wherein AP-1 family engagement promotes a progressive hypertrophic chondrocyte program.

To test this model further, we co-expressed *Fosl2* and *Jun*, or expressed TAM67 or a GFP control, in neonatal mouse primary chondrocytes. Ectopic expression of *Fosl2* and *Jun* downregulated expression of markers of proliferative and prehypertrophic chondrocytes (*Col2a1*, *Sox9*, *Sp7*, *Mef2c* and *Ihh*), but upregulated *Col10a1*, an early indicator of hypertrophic development (Fig. 5E); expression of *Mmp13*, a marker of the most mature mineralizing hypertrophic chondrocytes that do not show either Jun or Fosl2 activity (Fig. 1A,A′,B,B′,H), was unaltered on the ectopic expression of *Fosl2* and *Jun* (Fig. 5E). Ectopic expression of TAM67 exerted opposite effects on expression of these genes to those invoked by *Fosl2* and *Jun* (Fig. 5E). Next, we examined the effect of ectopic expression of *Fosl2* and *Jun* on the developing zebrafish skeleton using Tol2 transposase for transposon-mediated transgenesis in the zebrafish embryo (Fig. 5F). Ectopic expression resulted in premature mineralization of endochondral cartilage elements (Fig. 5G-I). By contrast, mineralization was delayed on ectopic expression of TAM67 (Fig. 5G-I). Together, these data support findings from earlier gain-of-function and dominant-negative approaches *in vitro* and *in vivo*.

To examine *Sox9* function in the hypertrophic program directly, we used an *Sp7* (also known as osterix)-driven CRE transgenic mouse strain (Rodda and McMahon, 2006) to remove *Sox9* activity specifically at the prehypertrophic transition, contrasting with other studies that have removed Sox9 from the columnar chondrocytes (Dy et al., 2012; Ikegami et al., 2011). Prehypertrophic chondrocyte-specific removal of *Sox9* led to an expansion of the prehypertrophic chondrocyte zone (Fig. S5A,B) and pronounced loss of *Col10a1*-expressing hypertrophic chondrocytes (Fig. S5C,D; see also S5C′,D′ for higher magnification), providing evidence in support of Sox9 action in promoting progressive development of hypertrophic chondrocytes. In this, *Col10a1* appears to be one likely shared target of Sox9 and Fosl2/Jun regulation from our primary ChIP-seq data (Fig. 2F) with strong binding to an *in vivo*-verified hypertrophic enhancer (Fig. 6A), transfection studies examining transcriptional responses in transfected primary rib chondrocytes (Fig. 6B), and data reviewed earlier (Gebhard et al., 2004; Leung et al., 2011; Li et al., 2011; Riemer et al., 2002).

To examine this possibility further, we tested the effects of Sox9 or Jun on reporter gene expression driven from the Sox9/Jun-bound *Col10a1* enhancer (Fig. S6). Individually, each factor upregulated reporter activity, and reporter activity was further enhanced when both Sox9 and Jun were transfected together (Fig. 6C, pGL-Col10WT-enh). Consistent with the direct DNA-dependent interaction of each factor, Sox9 and AP-1 were no longer able

to activate the reporter when their predicted binding sites were mutated (Fig. 6C, pGL-Col10SM-enh and pGL-Col10AM-enh). Collectively, these data suggest that *Col10a1* is one key, direct target upregulated by Sox9 and AP-1 in hypertrophic chondrocyte development.

DISCUSSION

Our data argue for a complex interplay between Sox9 and at least two AP-1 family members, Jun and Fosl2, in chondrocyte development. Whereas Jun binds a large array of DNA regions independently of Sox9, the strongest Jun-bound regions closely overlap with the large majority of Sox9 DNA targets in developing rib chondrocytes. Two distinct modes of Sox9 and AP-1 factor co-engagement were observed with distinct transcriptional consequences. Sox9 can form protein-protein complexes with Jun and Fosl2. At enhancers where direct binding of only Sox9 or AP-1 complexes is possible, protein-protein interactions attenuate the direct binding factor's transcriptional activity. By contrast, when Sox9 and AP-1 engage together through their cognate DNA-target sequence, their combined actions elevate expression above levels induced by either factor alone. Given our recent findings (Ohba et al., 2015) and those of other groups (Bhandari et al., 2012; Liu and Lefebvre, 2015; Oh et al., 2014, 2010) that the transcription of Sox9-specific chondrocyte targets is governed by integrating information from multiple independent enhancer elements, the overall impact of AP-1 factor activation on any given Sox9/AP-1 target gene is not easy to predict as it will reflect the combined action of multiple binding activities within any given enhancer and the integration of information from multiple enhancers; the inhibitory action of protein-protein interactions could function to fine-tune expression of target genes. However, the balance of the evidence herein suggests that the combined action of AP-1 factor input promotes a progressive hypertrophic chondrocyte program with Sox9. In addition, AP-1 family members other that Jun and Fosl2 may be expressed in proliferating chondrocytes and participate in Sox9-mediated gene regulation at the mitotic phase, although this study has not addressed this possibility. Extensive studies have linked AP-1 family action to bone formation, bone modeling, joint formation and intervertebral disc development (see Introduction). However, there is only limited prior evidence suggesting AP-1 action in chondrogenesis. Ectopic expression of Jun and JunD *in vitro* in chicken sternum chondrocytes has been reported to inhibit hypertrophic gene expression (Kameda et al., 1997). By contrast, *in vivo Fosl2* removal from mammalian chondrocytes is reported to reduce the hypertrophic chondrocyte zone and associated calcified matrix, consistent with a positive role in hypertrophic chondrocyte development (Karreth et al., 2004).

Though *Jun* mutants do display joint phenotypes we saw no obvious phenotype in the remainder of the neonatal skeleton (Kan and Tabin, 2013). By contrast, small molecule-mediated AP-1 factor inhibition provided evidence in favor of an AP-1 input enhancing hypertrophic development. However, the precise action of this small molecule inhibitor is unclear, as is the extent of AP-1 family member inhibition. RNA-seq analysis indicates multiple AP-1 family members are expressed in hypertrophic chondrocytes in addition to *Jun* and *Fosl2* as studied here. The potential for significant redundancy among family members precludes establishing a clear genetic resolution to the full potential of AP-1 family regulatory action in chondrocytes.

In contrast to AP-1 factors, Sox9 has been extensively studied in early chondrogenenesis. Sox9 is absolutely required for specification of mitotic chondrocytes (reviewed by Lefebvre, 2002). However, genetic studies have been less clear on the role
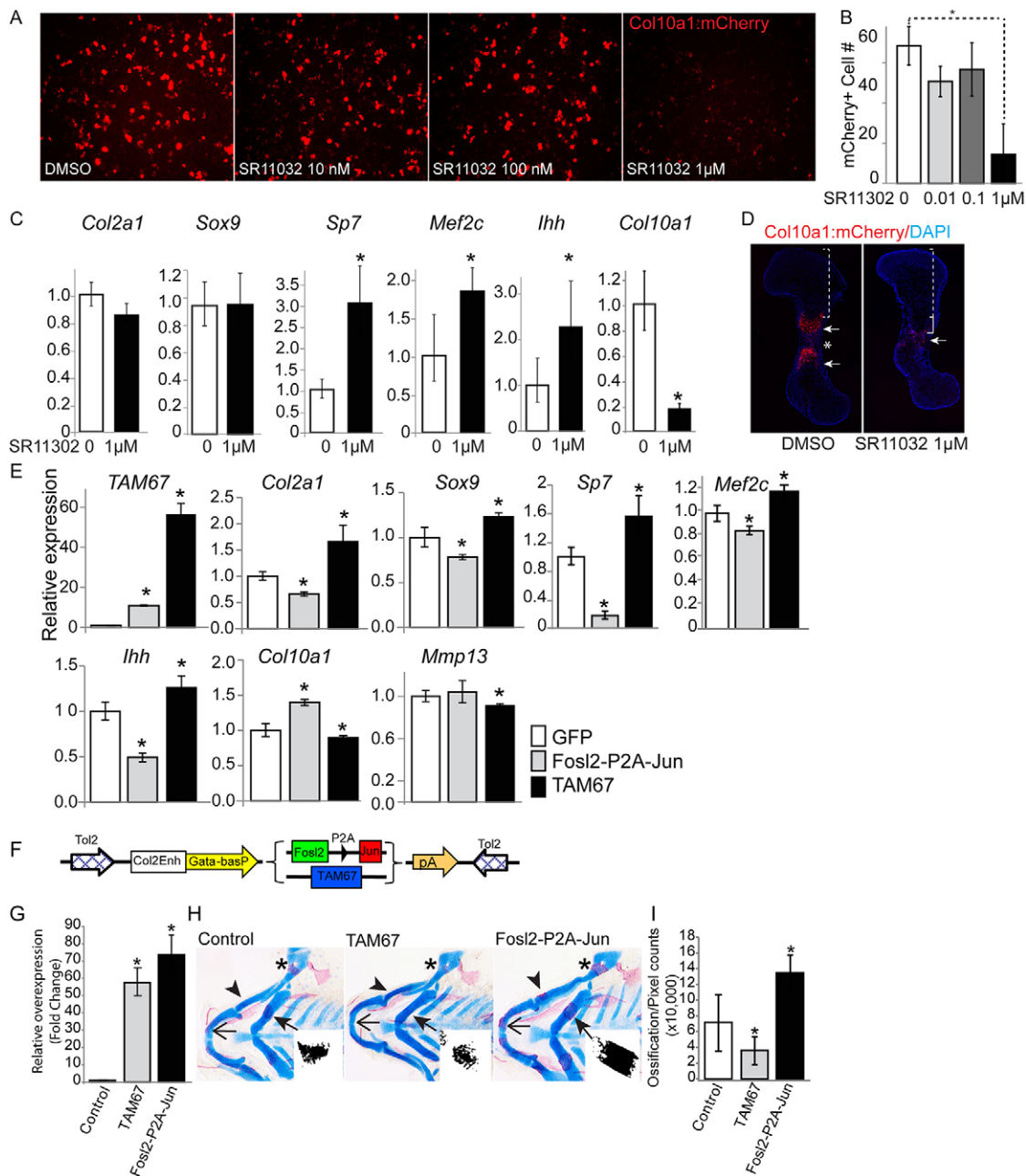
DEVELOPMENT

Fig. 5. AP-1 induces chondrocyte hypertrophy. (A,B) *Col10a1:mCherry* transgene expression in chondrocytes cultured with the AP-1 inhibitor SR11302. Primary rib chondrocytes isolated from *Col10a1:mCherry* transgenic mice were cultured for 10 days with SR11302 at the indicated concentrations in the presence of an insulin-transferrin-selenium (ITS) supplement with phosphate to induce hypertrophy. mCherry from the *Col10a1:mCherry* transgene indicates chondrocyte hypertrophy. Representative pictures of mCherry signal and quantitative data for mCherry-positive cells (biological triplicates) are shown in A and B, respectively. *$P<0.05$. (C) Expression of chondrocyte differentiation marker genes in the culture shown in A. Relative mRNA expression levels are determined by reverse transcription-quantitative polymerase chain reaction (RT-qPCR). *$P<0.05$. (D) Chondrocyte hypertrophy in femurs cultured with SR11302. Femurs isolated from E12.5 *Col10a1:mCherry* transgenic mice were cultured with 1 µM SR11302 for 5 days. mCherry highlights the hypertrophic chondrocyte domain, brackets indicate distance from articular surface to onset of mCherry-expressing hypertrophic domain. Arrows indicate the *Col10a1:mCherry*-expressing hypertrophic domain. Asterisk indicates the ossification domain. (E) mRNA expression of chondrocyte differentiation markers in cultured chondrocytes overexpressing *Fosl2* and *Jun* or TAM67. Primary mouse rib chondrocytes were infected with virus overexpressing *Fosl2*-P2A-*Jun*, TAM67 or GFP control and cultured for 3 days. Triplicate analysis of mRNA expression for the indicated genes analyzed by RT-qPCR. Primers for *TAM67* detected not only TAM67 but also full-length *Jun*, which enabled assessment of the ectopic expression of each factor. *Col2a1* and *Sox9* are broadly active in mitotic chondrocytes; *Sp7*, *Mef2c* and *Ihh* in prehypertrophic chondrocytes; and *Col10a1* and *Mmp13* in hypertrophic chondrocytes. *$P<0.05$ compared with the GFP control group. (F) A Tol2 transposase construct was used to introduce transgenes to ectopically express AP-1 factors (*Fosl2*-P2A-*Jun* transgene) or *TAM67* under the control of mouse *Col2a1* intron 6 enhancer (Ohba et al., 2015), which has been shown to direct robust transgene expression within zebrafish chondrocytes during skeletal development (Ohba et al., 2015). (G,H) Altered endochondral ossification in the pharyngeal arch of the 7-day zebrafish larva following overexpression of *Fosl2*-P2A-*Jun* and *TAM67*. The expression level of introduced genes was examined by RT-qPCR (G). Representative images of Alcian Blue/Alizarin Red staining are shown in H. Arrowheads, mineralization in palatoquadrate; arrows, mineralization in ceratohyal arch; asterisk, mineralization in hyosymplectic cartilage. Inset in each panel of H shows a representative Alizarin signal within the ceratohyal arch. (I) The histochemical signal in H was quantified using ImageJ (*n*=7 for each treatment). *$P<0.05$ comparing transgenic with stage-matched control groups. Error bars represent s.d.
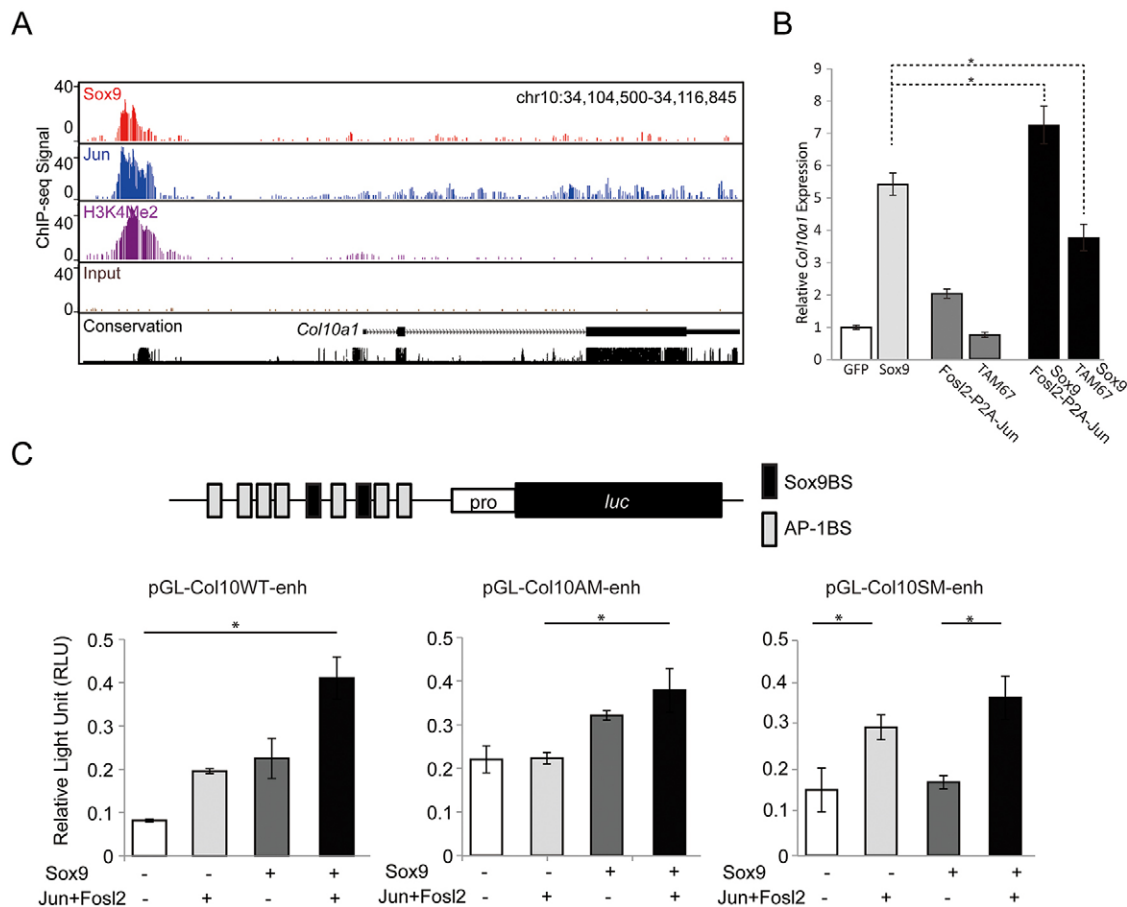
Fig. 6. Sox9 and AP-1 cooperatively induce the expression of *Col10a1*. (A) Screenshot of *Col10a1* genomic locus showing a conserved block (black trace) enriched for Sox9 (red) and Jun (blue) ChIP-seq signals and an H3K4Me2 enhancer mark (purple) compared with input controls (brown). Conservation plot indicates phastcons value (conservation among 30 vertebrate species). (B) The effect on *Col10a1* expression in primary rib chondrocyte culture following viral overexpression of *Sox9* with either *Fosl2*-P2A-*Jun* or *TAM67*. mRNA expression values were determined by RT-qPCR 3 days after viral infection. *y*-axis indicates relative expression value over *Gapdh* value, normalized to the control groups infected with GFP-expressing viruses. *$P<0.05$. (C) Reporter assay analysis in HEK293T cells of luciferase constructs carrying the conserved block of a *Col10a1* enhancer containing seven predicted AP-1 binding motifs and two Sox9 binding motifs. Wild-type enhancer construct (pGL-Col10WT-enh) and constructs with mutations to all AP-1 binding sites (pGL-Col10AM-enh) or all Sox9 binding sites (pGL-Col10SM-enh) were transfected with Sox9 and/or Jun and Fosl2 expression constructs. Relative expression of firefly luciferase was normalized to a *Renilla* luciferase internal control. *$P<0.05$. See also Fig. S6. Error bars represent s.d.

of Sox9 in later, post-mitotic, hypertrophic chondrocyte development. Early deletion of Sox9 from *Prrx1*- or *Col2a1*-expressing cells blocks initiation or ongoing chondrogenesis, respectively (Akiyama et al., 2002). Further, spatial and temporal refinement of Sox9 removal from chondrocytes has supported a continuing role in promoting the hypertrophic chondrocyte transition (Dy et al., 2012; Ikegami et al., 2011).

Interestingly, our data show that Sox9 nuclear levels are highest at the prehypertrophic boundary precisely where Jun and Fosl2 expression initiate. Further, Sox9 and AP-1 family members co-bind each other's cis-regulatory regions, suggesting that cross- and auto-regulatory interactions might contribute to their observed patterns of gene activity. Removing Sox9 activity at the point of the prehypertrophic transition *in vivo* demonstrated that *Sox9* is essential for the cellular progression to hypertrophic chondrocytes, consistent with the published studies discussed above. Further, drug-mediated attenuation of AP-1 factor activity blocked hypertrophic chondrocyte development, suggesting that both Sox9 and AP-1 have positive roles in the hypertrophic component of the endochondral skeletal program. One prominent co-regulated target in our study is *Col10a1*: Col10a1 activity in

primary chondrocytes *in vitro* depends directly on Sox9 and AP-1 factor engagement in agreement with transfection studies of AP-1 factors in cell culture (Gebhard et al., 2004) but contrasting with transgenic studies that show that loss of a single Sox9-binding site within the context of a *Col10a1* enhancer element results in premature activation of reporter in proliferating chondrocytes (Leung et al., 2011). The differences between these studies most likely reflect the limitation of analysis of single binding events in single enhancer elements where the *in vivo* picture is multiple binding events in multiple enhancer elements.

Previous studies have argued that Gli factors facilitate Sox9 inhibition of *Col10a1* expression in proliferating chondrocytes (Leung et al., 2011). Interestingly, hedgehog responsiveness, as indicated by upregulation of Ptch1 and Gli1 targets, is lost at the prehypertrophic chondrocyte boundary (St-Jacques et al., 1999). Thus, the hypertrophic transition may act as a regulatory switch point for Sox9 control of hypertrophic target gene activity removing negative interactions (Gli), and activating *de novo* AP-1 factors to promote hypertrophic gene activity with Sox9.

Parathyroid hormone-like hormone (Pthlh; also known as Pthrp) signaling through the Pthlh receptor is a key inhibitor of the

hypertrophic chondrocyte program (reviewed by Kronenberg, 2003). Pthlh is reported to induce AP-1 factors and enhance their DNA-binding activity *in vitro*, and dominant-negative forms of Fos have been reported to abolish Pthlh-mediated suppression of chondrocyte maturation in culture (Ionescu et al., 2001). In addition, Pthlh specifically activates Sox9 by phosphorylating Sox9 at serine 181 through protein kinase A exclusively in prehypertrophic chondrocytes, although the role of phosphorylated Sox9 has not been well studied (Huang et al., 2001).

Collectively, our *in vivo* and *in vitro* studies provide several lines of evidence supporting a direct ongoing role for Sox9 in the early stages of the hypertrophic program. Further, the data suggest that the actions of Sox9 in promoting the hypertrophic phase are augmented by the co-regulatory input of AP-1 family members at enhancer modules, a regulatory mode initiated on chondrocyte commitment to the hypertrophic program.

These studies suggest that the cell type-specific actions of Sox9 and AP-1 family members are crucially linked to the timing of chondrocyte development. Our Sox9 ChIP-seq analysis of primary chondrocytes reflects a mixed population of chondrocytes at different stages of chondrogenesis. Consequently, the exact timing of Sox9 action on a given enhancer is unclear and will require a significant technological improvement to be able to address *in vivo* given the small number of cells present within any skeletal element. However, the close concordance of Jun engagement at DNA targets with Sox9 and prehypertrophic-specific expression of Jun suggest that Jun interactions follow those of Sox9. Interestingly, Jun binds to many more genomic regions than does Sox9, but these 'Jun-only'-associated regions do not display an active enhancer signature.

In this view, Sox9 likely provides the chondrocyte-context to a Jun regulatory input in chondrogenesis. Jun binds to a broad array of enhancers, many of which, such as those regulating *Col2a1*, were active under Sox9 control at an earlier stage (Ohba et al., 2015), whereas others, such as *Col10a1*, switch on in hypertrophic cells. As most of the early-activated enhancers remain active in the early phase of hypertrophic chondrocyte development, Jun and Fosl2 complexes formed at the hypertrophic transition could provide an additional layer of regulatory input into these early-initiating enhancers while providing *de novo* activating input into *Col10a1* enhancers.

Although most of the Jun-Sox9 shared peak regions can be accounted for by a direct interaction of at least one of these factors, a small number (16%) of them show no readily identifiable Sox9 or AP-1 motif. This may reflect degeneracy of target sites. Alternatively, these data may point to additional interactions with other transcriptional regulators. In line with this, we recovered additional motifs within the Jun ChIP-seq dataset that might reflect an indirect association of Jun to the chondrocyte genome through engagement with other transcriptional regulatory factors. Of note, our analysis of Sox9-binding sites recovered significant enrichment for Runx-, Nfat-, Ets- and AT-rich homeodomain protein-binding motifs (Ohba et al., 2015). Of these possible co-operating factors, Runx2 is known to play an essential role in hypertrophic chondrocyte development and is normally targeted by Jun (Ding et al., 2012; Li et al., 2011; Papachristou et al., 2005; Yoshida et al., 2004) and Runx2 is reported to upregulate both *Col10a1* and *Sox9* in the *Col10a1* expression domain (Ding et al., 2012), suggesting an interacting, positive regulatory loop. However, counter evidence suggests Sox9 upregulates *Bapx1* (*Nkx3-2*), a negative regulator of *Runx2* (Yamashita et al., 2009). Further, protein-protein interactions have been documented between Sox9 and Runx2 that are reported to attenuate Sox9-mediated transcriptional activation of target genes, suggesting a complex regulatory interplay (Zhou et al., 2006).

Future studies developing strategies to incorporate Runx2, Bapx1, Mef2c and other transcriptional regulators of the hypertrophic program will help to decipher the regulatory logic of this key developmental event in mammalian skeletogenesis.

MATERIALS AND METHODS
Ethics statement
All experiments in this study were carried out in strict accordance with the recommendation in the Guide for the Care and Use of Laboratory Animals of the National Institutes of Health, USA. The procedures were approved by the Institutional Animal Care and Use Committee of The University of Southern California (IACUC # 11892).

In situ hybridization
Cryosections of postnatal day 1 (P1) Swiss Webster mouse skeletal samples were subjected to *in situ* hybridization with digoxigenin-labeled riboprobes. See supplementary Materials and Methods for further details of sample preparation and riboprobes.

Chromatin immunoprecipitation (ChIP), ChIP-seq library construction, and reChIP
ChIP was performed on P1 mouse rib chondrocytes as previously described (Ohba et al., 2015), using specific antibodies against Jun. ChIP-seq libraries were constructed using ThruPLEX DNA-seq Kit (Rubicon Genomics, R400429). See supplementary Materials and Methods for further details of chromatin preparation, antibodies, and library construction.

ReChIP was performed by sequential precipitations of chromatin using specific antibodies against Sox9 and Jun. DNA was analyzed by conventional polymerase chain reaction (PCR) and quantitative PCR (qPCR). See supplementary Materials and Methods for further details of the reChIP procedure, antibodies, and PCR primers.

ChIP-seq data analysis
Sequencing was performed in the Epigenome Center of the University of Southern California. Data were analyzed as previously described (Ohba et al., 2015); alignment of sequence reads, peak calling, *de novo* motif analysis, and gene ontology analysis of genes associated with obtained peaks were performed using ELAND, CisGenome software (Ji et al., 2008; Jiang et al., 2010), MEME-ChIP (Bailey et al., 2009), and GREAT (McLean et al., 2010) and DAVID (Huang da et al., 2009), respectively. See supplementary Materials and Methods for further details of these analyses.

Expression profiling
Ribs were digested with collagenase D from P1 *Col10a1:mCherry* transgenic mice. Fluorescence-activated cell sorting was performed to isolate RNA from 100,000 mCherry-positive chondrocytes. Sequencing was performed as mentioned above. Sequence reads were mapped with TopHat2 and quantified with Partek software. See supplementary Materials and Methods for further details of RNA isolation and sequencing library construction.

Plasmid construction
Plasmids expressing genes of interest were constructed by cloning of cDNA into mammalian expression vectors; cDNA was obtained by a PCR-based strategy. Luciferase reporter constructs were generated by cloning of annealed oligonucleotides into luciferase reporter vectors. Retroviral vectors were based on the pMX vector platform, and viral particles were produced in plat-E cells. See supplementary Materials and Methods for further details of cloning procedures.

Co-immunoprecipitation (co-IP), SDS-PAGE and western blotting
Nuclear extracts of HEK293T cells transfected with plasmids were subjected to co-IP, followed by SDS-PAGE of precipitated materials and western blotting. See supplementary Materials and Methods for further details of nuclear extract preparation, co-IP reaction, immunostaining of blotted membranes, and image acquisition.

DEVELOPMENT

Mouse primary chondrocyte culture

Chondrocytes were obtained from ribs of P1 Swiss Webster mice or *Col10a1:mCherry* transgenic mice by enzymatic digestion and subjected to cultures. mRNA expression was analyzed by reverse transcription (RT)-qPCR. See supplementary Materials and Methods for further details of cell isolation, cultures and mRNA expression analysis.

Mouse femur explant culture

Femurs were obtained from embryonic day (E) 12.5 *Col10a1:mCherry* transgenic mice and cultured with 1 µM of SR11302 (R&D Systems, 2476) or in DMSO in α-MEM/10% fetal bovine serum with antibiotics (penicillin-streptomycin; Sigma-Aldrich, P4333). Culture medium was changed daily with fresh SR11302 or DMSO.

Zebrafish assays

For zebrafish overexpression, Fosl2-P2A-Jun or TAM67 cDNAs, and E1 Col2a1 enhancer-reporter constructs were cloned into a Tol2 construct containing a zebrafish *gata2* basal promoter (Kwan et al., 2007). Forty nanograms of each overexpression construct was injected together with 50 ng of Tol2 transposase into 1-cell-stage fertilized zebrafish embryos. The skeletal pattern was visualized by Alcian Blue and Alizarin Red staining of developing zebrafish (Walker and Kimmel, 2007). The extent of mineralization was quantified by measuring the red (Alizarin Red) pixels using ImageJ analysis of skeletal images.

Luciferase reporter assays

Luciferase and effector constructs were transfected into HEK293T cells with FuGENE-6 transfection reagent (Promega, E2691). After 48 h, luciferase activities were measured with the Dual-Glo Luciferase Reporter Assay System (Promega, E2920). For transfection of cells cultured on 96-well culture plates, 100 ng of total DNA was mixed with 0.3 µl FuGENE-6 reagent in DMEM per well. In the DNA mix, 5 ng of a thymidine kinase promoter driving a *Renilla* control construct was mixed with 10 ng of the experimental firefly luciferase construct. Up to 5 ng of Sox9-expressing construct and up to equal amounts of Fosl2 construct and Jun construct were used as effectors (up to 70 ng combined). A GFP construct was added to make up each DNA transfection to 100 ng DNA per well.

Immunostaining

Cryosections of E16.5 *Sp7Cre;Sox9*^{+/+} or *Sp7Cre;Sox9*[flox/flox] limbs were subjected to immunostaining using specific antibodies, in combination with secondary antibodies. See supplementary Materials and Methods for further details of sample preparation, antibodies and staining procedures.

Data availability

ChIP-seq and RNA-seq data are available in NCBI Gene Expression Omnibus (GEO) under accession number GSE73372 (http://www.ncbi.nlm.nih.gov/geo/query/acc.cgi?acc=GSE73372).

Supplementary information

Supplementary information available online at
http://dev.biologists.org/lookup/doi/10.1242/dev.134502.supplemental

References

Akiyama, H. and Lefebvre, V. (2011). Unraveling the transcriptional regulatory machinery in chondrogenesis. *J. Bone Miner. Metab.* **29**, 390-395.

Akiyama, H., Chaboissier, M.-C., Martin, J. F., Schedl, A. and de Crombrugghe, B. (2002). The transcription factor Sox9 has essential roles in successive steps of the chondrocyte differentiation pathway and is required for expression of Sox5 and Sox6. *Genes Dev.* **16**, 2813-2828.

Akiyama, H., Kim, J.-E., Nakashima, K., Balmes, G., Iwai, N., Deng, J. M., Zhang, Z., Martin, J. F., Behringer, R. R., Nakamura, T. et al. (2005). Osteo-chondroprogenitor cells are derived from Sox9 expressing precursors. *Proc. Natl. Acad. Sci. USA* **102**, 14665-14670.

Bailey, T. L., Boden, M., Buske, F. A., Frith, M., Grant, C. E., Clementi, L., Ren, J., Li, W. W. and Noble, W. S. (2009). MEME SUITE: tools for motif discovery and searching. *Nucleic Acids Res.* **37**, W202-W208.

Behrens, A., Haigh, J., Mechta-Grigoriou, F., Nagy, A., Yaniv, M. and Wagner, E. F. (2003). Impaired intervertebral disc formation in the absence of Jun. *Development* **130**, 103-109.

Bhandari, R. K., Haque, M. M. and Skinner, M. K. (2012). Global genome analysis of the downstream binding targets of testis determining factor SRY and SOX9. *PLoS ONE* **7**, e43380.

Bi, W., Deng, J. M., Zhang, Z., Behringer, R. R. and de Crombrugghe, B. (1999). Sox9 is required for cartilage formation. *Nat. Genet.* **22**, 85-89.

Bi, W., Huang, W., Whitworth, D. J., Deng, J. M., Zhang, Z., Behringer, R. R. and de Crombrugghe, B. (2001). Haploinsufficiency of Sox9 results in defective cartilage primordia and premature skeletal mineralization. *Proc. Natl. Acad. Sci. USA* **98**, 6698-6703.

Brown, P. H., Alani, R., Preis, L. H., Szabo, E. and Birrer, M. J. (1993). Suppression of oncogene-induced transformation by a deletion mutant of c-jun. *Oncogene* **8**, 877-886.

Chambers, D., Young, D. A., Howard, C., Thomas, J. T., Boam, D. S., Grant, M. E., Wallis, G. A. and Boot-Handford, R. P. (2002). An enhancer complex confers both high-level and cell-specific expression of the human type X collagen gene. *FEBS Lett.* **531**, 505-508.

Cheng, A. and Genever, P. G. (2010). SOX9 determines RUNX2 transactivity by directing intracellular degradation. *J. Bone Miner. Res.* **25**, 2680-2689.

Chung, U.-I., Schipani, E., McMahon, A. P. and Kronenberg, H. M. (2001). Indian hedgehog couples chondrogenesis to osteogenesis in endochondral bone development. *J. Clin. Invest.* **107**, 295-304.

Ding, M., Lu, Y., Abbassi, S., Li, F., Li, X., Song, Y., Geoffroy, V., Im, H.-J. and Zheng, Q. (2012). Targeting Runx2 expression in hypertrophic chondrocytes impairs endochondral ossification during early skeletal development. *J. Cell. Physiol.* **227**, 3446-3456.

Dy, P., Wang, W., Bhattaram, P., Wang, Q., Wang, L., Ballock, R. T. and Lefebvre, V. (2012). Sox9 directs hypertrophic maturation and blocks osteoblast differentiation of growth plate chondrocytes. *Dev. Cell* **22**, 597-609.

Eferl, R. and Wagner, E. F. (2003). AP-1: a double-edged sword in tumorigenesis. *Nat. Rev. Cancer* **3**, 859-868.

Fanjul, A., Dawson, M. I., Hobbs, P. D., Jong, L., Cameron, J. F., Harlev, E., Graupner, G., Lu, X.-P. and Pfahl, M. (1994). A new class of retinoids with selective inhibition of AP-1 inhibits proliferation. *Nature* **372**, 107-111.

Foster, J. W. (1996). Mutations in SOX9 cause both autosomal sex reversal and campomelic dysplasia. *Acta Paediatr. Jpn.* **38**, 405-411.

Gebhard, S., Poschl, E., Riemer, S., Bauer, E., Hattori, T., Eberspaecher, H., Zhang, Z., Lefebvre, V., de Crombrugghe, B. and von der Mark, K. (2004). A highly conserved enhancer in mammalian type X collagen genes drives high levels of tissue-specific expression in hypertrophic cartilage in vitro and in vivo. *Matrix Biol.* **23**, 309-322.

Giordano, J., Prior, H. M., Bamforth, J. S. and Walter, M. A. (2001). Genetic study of SOX9 in a case of campomelic dysplasia. *Am. J. Med. Genet.* **98**, 176-181.

Hess, J., Hartenstein, B., Teurich, S., Schmidt, D., Schorpp-Kistner, M. and Angel, P. (2003). Defective endochondral ossification in mice with strongly compromised expression of JunB. *J. Cell Sci.* **116**, 4587-4596.

Huang, W., Chung, U.-I., Kronenberg, H. M. and de Crombrugghe, B. (2001). The chondrogenic transcription factor Sox9 is a target of signaling by the parathyroid hormone-related peptide in the growth plate of endochondral bones. *Proc. Natl. Acad. Sci. USA* **98**, 160-165.

DEVELOPMENT

Ikeda, T., Kamekura, S., Mabuchi, A., Kou, I., Seki, S., Takato, T., Nakamura, K., Kawaguchi, H., Ikegawa, S. and Chung, U.-I. (2004). The combination of SOX5, SOX6, and SOX9 (the SOX trio) provides signals sufficient for induction of permanent cartilage. *Arthritis Rheum.* **50**, 3561-3573.

Ikegami, D., Akiyama, H., Suzuki, A., Nakamura, T., Nakano, T., Yoshikawa, H. and Tsumaki, N. (2011). Sox9 sustains chondrocyte survival and hypertrophy in part through Pik3ca-Akt pathways. *Development* **138**, 1507-1519.

Ionescu, A. M., Schwarz, E. M., Vinson, C., Puzas, J. E., Rosier, R., Reynolds, P. R. and O'Keefe, R. J. (2001). PTHrP modulates chondrocyte differentiation through AP-1 and CREB signaling. *J. Biol. Chem.* **276**, 11639-11647.

Ji, H., Jiang, H., Ma, W., Johnson, D. S., Myers, R. M. and Wong, W. H. (2008). An integrated software system for analyzing ChIP-chip and ChIP-seq data. *Nat. Biotechnol.* **26**, 1293-1300.

Jiang, H., Wang, F., Dyer, N. P. and Wong, W. H. (2010). CisGenome Browser: a flexible tool for genomic data visualization. *Bioinformatics* **26**, 1781-1782.

Kameda, T., Watanabe, H. and Iba, H. (1997). C-Jun and JunD suppress maturation of chondrocytes. *Cell Growth Differ.* **8**, 495-503.

Kan, A. and Tabin, C. J. (2013). c-Jun is required for the specification of joint cell fates. *Genes Dev.* **27**, 514-524.

Kan, A., Ikeda, T., Saito, T., Yano, F., Fukai, A., Hojo, H., Ogasawara, T., Ogata, N., Nakamura, K., Chung, U.-I. et al. (2009). Screening of chondrogenic factors with a real-time fluorescence-monitoring cell line ATDC5-C2ER: identification of sorting nexin 19 as a novel factor. *Arthritis Rheum.* **60**, 3314-3323.

Karreth, F., Hoebertz, A., Scheuch, H., Eferl, R. and Wagner, E. F. (2004). The AP1 transcription factor Fra2 is required for efficient cartilage development. *Development* **131**, 5717-5725.

Kronenberg, H. M. (2003). Developmental regulation of the growth plate. *Nature* **423**, 332-336.

Kwok, C., Weller, P. A., Guioli, S., Foster, J. W., Mansour, S., Zuffardi, O., Punnett, H. H., Dominguez-Steglich, M. A., Brook, J. D., Young, I. D. et al. (1995). Mutations in SOX9, the gene responsible for Campomelic dysplasia and autosomal sex reversal. *Am. J. Hum. Genet.* **57**, 1028-1036.

Lefebvre, V. (2002). Toward understanding the functions of the two highly related Sox5 and Sox6 genes. *J. Bone Miner. Metab.* **20**, 121-130.

Lefebvre, V. and Dvir-Ginzberg, M. (2016). SOX9 and the many facets of its regulation in the chondrocyte lineage. *Connect. Tissue Res.* (in press).

Leung, V. Y. L., Gao, B., Leung, K. K. H., Melhado, I. G., Wynn, S. L., Au, T. Y. K., Dung, N. W. F., Lau, J. Y. B., Mak, A. C. Y., Chan, D. et al. (2011). SOX9 governs differentiation stage-specific gene expression in growth plate chondrocytes via direct concomitant transactivation and repression. *PLoS Genet.* **7**, e1002356.

Li, F., Lu, Y., Ding, M., Napierala, D., Abbassi, S., Chen, Y., Duan, X., Wang, S., Lee, B. and Zheng, Q. (2011). Runx2 contributes to murine Col10a1 gene regulation through direct interaction with its cis-enhancer. *J. Bone Miner. Res.* **26**, 2899-2910.

Liu, C.-F. and Lefebvre, V. (2015). The transcription factors SOX9 and SOX5/SOX6 cooperate genome-wide through super-enhancers to drive chondrogenesis. *Nucleic Acids Res.* **43**, 8183-8203.

Maye, P., Fu, Y., Butler, D. L., Chokalingam, K., Liu, Y., Floret, J., Stover, M. L., Wenstrup, R., Jiang, X., Gooch, C. et al. (2011). Generation and characterization of Col10a1-mcherry reporter mice. *Genesis* **49**, 410-418.

McLean, C. Y., Bristor, D., Hiller, M., Clarke, S. L., Schaar, B. T., Lowe, C. B., Wenger, A. M. and Bejerano, G. (2010). GREAT improves functional interpretation of cis-regulatory regions. *Nat. Biotechnol.* **28**, 495-501.

Mori-Akiyama, Y., Akiyama, H., Rowitch, D. H. and de Crombrugghe, B. (2003). Sox9 is required for determination of the chondrogenic cell lineage in the cranial neural crest. *Proc. Natl. Acad. Sci. USA* **100**, 9360-9365.

Oh, C.-D., Maity, S. N., Lu, J.-F., Zhang, J., Liang, S., Coustry, F., de Crombrugghe, B. and Yasuda, H. (2010). Identification of SOX9 interaction sites in the genome of chondrocytes. *PLoS ONE* **5**, e10113.

Oh, C.-D., Lu, Y., Liang, S., Mori-Akiyama, Y., Chen, D., de Crombrugghe, B. and Yasuda, H. (2014). SOX9 regulates multiple genes in chondrocytes, including genes encoding ECM proteins, ECM modification enzymes, receptors, and transporters. *PLoS ONE* **9**, e107577.

Ohba, S., He, X., Hojo, H. and McMahon, A. P. (2015). Distinct transcriptional programs underlie Sox9 regulation of the mammalian chondrocyte. *Cell Rep.* **12**, 229-243.

Outani, H., Okada, M., Yamashita, A., Nakagawa, K., Yoshikawa, H. and Tsumaki, N. (2013). Direct induction of chondrogenic cells from human dermal fibroblast culture by defined factors. *PLoS ONE* **8**, e77365.

Papachristou, D. J., Papachristou, G. I., Papaefthimiou, O. A., Agnantis, N. J., Basdra, E. K. and Papavassiliou, A. G. (2005). The MAPK-AP-1/-Runx2 signalling axes are implicated in chondrosarcoma pathobiology either independently or via up-regulation of VEGF. *Histopathology* **47**, 565-574.

Riemer, S., Gebhard, S., Beier, F., Poschl, E. and von der Mark, K. (2002). Role of c-fos in the regulation of type X collagen gene expression by PTH and PTHrP: localization of a PTH/PTHrP-responsive region in the human COL10A1 enhancer. *J. Cell Biochem.* **86**, 688-699.

Rodda, S. J. and McMahon, A. P. (2006). Distinct roles for Hedgehog and canonical Wnt signaling in specification, differentiation and maintenance of osteoblast progenitors. *Development* **133**, 3231-3244.

St-Jacques, B., Hammerschmidt, M. and McMahon, A. P. (1999). Indian hedgehog signaling regulates proliferation and differentiation of chondrocytes and is essential for bone formation. *Genes Dev.* **13**, 2072-2086.

Wagner, E. F. (2002). Functions of AP1 (Fos/Jun) in bone development. *Ann. Rheum. Dis.* **61** Suppl. 2, ii40-ii42.

Wagner, E. F. and Eferl, R. (2005). Fos/AP-1 proteins in bone and the immune system. *Immunol. Rev.* **208**, 126-140.

Yamashita, S., Andoh, M., Ueno-Kudoh, H., Sato, T., Miyaki, S. and Asahara, H. (2009). Sox9 directly promotes Bapx1 gene expression to repress Runx2 in chondrocytes. *Exp. Cell Res.* **315**, 2231-2240.

Yoshida, C. A., Yamamoto, H., Fujita, T., Furuichi, T., Ito, K., Inoue, K.-I., Yamana, K., Zanma, A., Takada, K., Ito, Y. et al. (2004). Runx2 and Runx3 are essential for chondrocyte maturation, and Runx2 regulates limb growth through induction of Indian hedgehog. *Genes Dev.* **18**, 952-963.

Zheng, Q., Keller, B., Zhou, G., Napierala, D., Chen, Y., Zabel, B., Parker, A. E. and Lee, B. (2009). Localization of the cis-enhancer element for mouse type X collagen expression in hypertrophic chondrocytes in vivo. *J. Bone Miner. Res.* **24**, 1022-1032.

Zhou, G., Zheng, Q., Engin, F., Munivez, E., Chen, Y., Sebald, E., Krakow, D. and Lee, B. (2006). Dominance of SOX9 function over RUNX2 during skeletogenesis. *Proc. Natl. Acad. Sci. USA* **103**, 19004-19009.

SUPPLEMENTARY MATERIALS AND METHODS

***In situ* hybridization**

Postnatal day 1 (P1) Swiss Webster mice skeletal samples were isolated and fixed in 4 % paraformaldehyde (PFA)/PBS overnight at 4 °C and then soaked in 30% sucrose/PBS overnight at 4 °C. After embedded in OCT compound, cryosections were generated at 10 μm thickness. *In situ* RNA hybridization was carried out as previously described (Eberhart et al., 2008). DNA templates for riboprobes were obtained from embryonic day (E) 18.5 mouse limb cDNA by PCR using the following primers: *Jun*-F, gaacttgactggttgcgaca; *Jun*-R, gaggttgggggctacttttc; *Fols2*-F, cgttggtctccaccagtttt; *Fosl2*-R, cttggcttgaggcgataaag; *Col1α1*-F, gcccgaaccccaaggaaaagaagc; *Col1α1*-R, cagattggggtggagggagttaca; *Col10α1*-F, ttctgctgctaatgttcttgacc; *Col10α1*-R, gggatgaagtattgtgtcttggg. PCR products were cloned into pGEMT easy TA cloning vector (Promega, A1360), and their sequences were verified. Plasmid DNA was linearized by enzymatic digestion downstream of insert DNA and antisense riboprobes were synthesized *in vitro* using RNA labeling kit (Roche, 11175025910) according to the manufacture's instruction.

Chromatin immunoprecipitation (ChIP), ChIP-seq library construction, and re-ChIP

P1 mouse primary rib chondrocytes were isolated by collagenase D digestion (see Mouse primary chondrocyte culture section). Isolated cells were immediately cross-linked with 1% formaldehyde for 10 minutes at room temperature, then 0.125 M Glycine was added to quench formaldehyde. About 20 million cells were used for one ChIP reaction. Chromatin preparation and ChIP was performed as described (Vokes et al., 2007). Chromatin was sonicated by 10 sessions of 30 pulses (1 sec on and 1 sec off) at 50% amplitude using the Branson sonifier 250D. 100 μL of Dynabeads M-280 Sheep anti-Rabbit IgG (Life Technologies, 11203D) was combined with 9 μg of anti-Jun antibodies (Abcam, ab31419). ChIP-seq libraries were constructed from input DNA as well as ChIP DNA using ThruPLEX® DNA-seq Kit (Rubicon Genomics, R400429) according to the manufacturer's instruction. An 18-cycle pre-amplification step was performed on barcoded DNA samples.

For re-ChIP, chromatin was prepared as above. After the first ChIP using 100 μL of Dynabeads M-280 Sheep anti-Rabbit IgG coupled with 9 μg of anti-Sox9 antibodies (Millipore, AB5535), beads were washed three times with the RIPA buffer (1% NP-40; 0.7% sodium deoxycholate; 1 mM EDTA; 50 mM HEPES-KOH, pH 7.5; and 500 mM LiCl) and once with the TE buffer. Beads were incubated in 15 mM DTT for 30 minutes at 37 °C, and eluates were then diluted 30-fold with the ChIP buffer (1 mM EDTA, 0.5 mM EGTA, 10 mM Tris, 130 mM NaCl, 0.13% sodium deoxycholate, and 1.3% Triton-X100). The second ChIP was performed using 100 μL of Dynabeads M-280 Sheep anti-Rabbit IgG coupled with 9 μg of anti-Jun antibodies (Abcam, ab31419). After washed three times with the RIPA buffer and once with the TE buffer, beads were incubated in the elution buffer (50 mM Tris, 10 mM EDTA, and 1% SDS) for 15 minutes at 65 °C. Reverse crosslink and recovery of DNA was performed as described (Vokes et al., 2007). DNA was analyzed by amplifying the following regions with conventional PCR and quantitative PCR (see also Fig. 3 E and F): chr15:97857031-97857184 (Sox9-AP-1-shared peaks with Sox9 and AP-1 motifs around the *Col2α1* gene; forward, 5'-gaggctgtgtatttttgtcatgg-3'; reverse, 5'-gtgcctcctctaacagagactca-3'), chr10:34076498-34076672 (Sox9-AP-1-shared

peaks with Sox9 and AP-1 motifs around the *Col10α1* gene; forward, 5'-cactgtagtgtctaatgcccaca-3'; reverse, 5'-gctcctttgacactttaatcctc-3'), chr15:97856092-97856262 (Sox9-AP-1-shared peaks only with Sox9 motif around the *Col2α1* gene; forward, 5'-cttctctgcaaagagtgctgtgt-3'; reverse, 5'-gctgcttttctgtcactgctaat-3'), chr10:34062970-34063158 (Sox9-AP-1-shared peaks only with Sox9 motif around the *Col10α1* gene; forward, 5'-aatctgccagtgaatgagtgaat-3'; reverse, 5'-tccaagagagatcccagtaaaca-3'), and chr15:97839448-97839608 (Sox9-only peak with Sox9 motif around the *Col2α1* gene; forward, 5'-ctttcaaggcatgtttgtgtttt-3'; reverse, 5'-attcttaatgctgtttgcctttg-3'). Gel images from the conventional PCR were captured FAS III and DIGITAL IMAGE STOCKER DS-1000 (TOYOBO).

ChIP-seq data analysis
Sequence reads (the first 25 bp) were aligned to the mouse genome mm9 by ELAND. Peak calling was performed by two-sample analysis on CisGenome software (Ji et al., 2008; Jiang et al., 2010) with a p-value cutoff of 10^{-5} by comparing with the input control. Peaks with an FDR<0.01 were used. Motif enrichments were performed by de novo motif analysis tool in Cisgenome and by MEME-ChIP (Bailey et al., 2009) on a 100bp window at top 500 peak centers. Cisgenome motif recovery searches show the enrichment of top 10 motifs following 3 independent rounds of motif discovery. MEME-CHIP search was run by default setting on the web application. Enriched motifs were mapped to peak centers. GREAT and DAVID GO analysis followed published guidelines (Huang da et al., 2009; McLean et al., 2010).

Expression profiling
Ribs were dissected from P1 *Col10α1:mCherry* transgenic mice, digested with Collagenase D then FACS sorted to isolate hypertrophic chondrocytes. Total RNA was extracted from 100,000 mCherry positive chondrocytes (RNeasy Micro Kit; Qiagen, 74004) with DNaseI digestion. Sequencing libraries were constructed with Truseq Stranded mRNA Sample Prep Kit (Illumina, RS-122-2101) according to the manufacturer's instruction using biological triplicates of polyA selected mRNA (starting pool of 100 ng total RNA). NextSeq sequencing was performed in the Epigenome Center of USC. Sequence reads were mapped with Tophat2 and quantified with Partek software. The nearest genes to the mouse rib Sox9 ChIP-seq products were matched for expression analysis.

Plasmids construction
To construct plasmids expressing mouse *Jun* and its derivative TAM67, and mouse *Fosl2*, their coding sequences were amplified by polymerase chain reaction (PCR) using Platinum Pfx DNA Polymerase (Life Technologies, 11708013) and cloned into pcDNA3.1(-) (Life Technologies, V795-20) with XbaI and EcoRI sites. Primers used in the PCR are as follows:
XbaI-Kozak-Myc-Jun_forward, 5'-actgtctagagccgccatggcatcaatgcagaagctgatctcagaggaggacctgactgcaaagatggaaacgacc-3'; EcoRI-Stop-Jun_reverse, 5'-actggaattctcaaaacgtttgcaactgctgcg-3'; XbaI-Kozak-Myc-TAM67_forward, 5'-actgtctagagccgccatggcatcaatgcagaagctgatctcagaggaggacctgagccagaacacgcttcccag-3'; EcoRI-Stop-TAM67_reverse, 5'-actggaattctcaaaacgtttgcaactgctgcg-3'; XbaI-Kozak-HA-Fosl2_forward: 5'-

actgtctagagccgcc<u>atgtacccatacgatgttccagattacgct</u>taccaggattatcccgggaac-3'; EcoRI-<u>Stop</u>-Fosl2_reverse: 5'-actggaattc<u>tta</u>cagggctagaagtgtgggg-3'.

To construct plasmids expressing human *SOX9* tagged with a Biotin-3xFLAG sequence, *SOX9* coding sequence was amplified by PCR using the following primers and cloned into pcDNA3.1(-) with XhoI and BamHI sites: XhoI-SOX9_forward, 5'-atgcctcgagatggatctcctggacccctt-3'; BamHI-SOX9_reverse, 5'-atgcggatccaggtcgagtgagctgtgtgt-3'. The biotin-3xFLAG sequence (Zhang et al., 2013) was then cloned at the c-terminus of the SOX9 with BamHI and HindIII sites. Deletion mutants of *Jun* and *SOX9* were generated by PCR-based strategies using Platinum Pfx DNA Polymerase (Life Technologies, 11708013).

A luciferase reporter construct driven by 4 copies of a 48-bp *COL2A1* intron 1 enhancer was provided by Drs. Toshiyuki Ikeda and Taku Saito (The University of Tokyo, Tokyo, Japan) (Kan et al., 2009). To make 3 x Col9a1BS, 7 x AP1BS and 3xCol9a1BS+7xAP1BS constructs, the following forward and reverse oligos were synthesized and annealed:

3xCol9Sox9+7xAp1-BglII-HindIII-F,

GATCTtgaaagagcccactgttGCTGAGCTGTtgaaagagcccactgttCAGAGGGAAGtgaaagagcccactgttcctgagctcTGAGTCAGTGACTCAGTGAGTCAGTGACTCAGTGAGTCAGTGACTCAgtggcctcggcggccagcttagacactAGAGGGTATATAATGGAAGCTCGACTTCCAGcttggcA;

3xCol9Sox9+7xAp1-BglII-HindIII-R,

AGCTTgccaagCTGGAAGTCGAGCTTCCATTATATACCCTCTagtgtctaagctggccgccgaggccacTGAGTCACTGACTCACTGAGTCACTGACTCACTGAGTCACTGACTCAgagctcaggaacagtgggctctttcaCTTCCCTCTGaacagtgggctctttcaACAGCTCAGCaacagtgggctctttcaA;

3xCol9Sox9-BglII-HindIII-F,

GATCTtgaaagagcccactgttGCTGAGCTGTtgaaagagcccactgttCAGAGGGAAGtgaaagagcccactgttcctgagctcTTAGGAAGTTACCCTGTTAGGAAGTTACCCTGTTAGGAAGTTACCCTgtggcctcggcggccagcttagacactAGAGGGTATATAATGGAAGCTCGACTTCCAGcttggcA;

3xCol9Sox9-BglII-HindIII-R,

AGCTTgccaagCTGGAAGTCGAGCTTCCATTATATACCCTCTagtgtctaagctggccgccgaggccacAGGGTAACTTCCTAACAGGGTAACTTCCTAACAGGGTAACTTCCTAAgagctcaggaacagtgggctctttcaCTTCCCTCTGaacagtgggctctttcaACAGCTCAGCaacagtgggctctttcaA;

7xAp1-BglII-HindIII-F,

GATCTcctgagctcTGAGTCAGTGACTCAGTGAGTCAGTGACTCAGTGAGTCAGTGACTCAgtggcctcggcggccagcttagacactAGAGGGTATATAATGGAAGCTCGACTTCCAGcttggcA;

7xAp1-BglII-HindIII-R,

AGCTTgccaagCTGGAAGTCGAGCTTCCATTATATACCCTCTagtgtctaagctggccgccgaggccacTGAGTCACTGACTCACTGAGTCACTGACTCACTGAGTCACTGACTCAgagctcaggA.

Equal concentrations (50 μM) of forward and reverse oligos were heated in boiling water for 3 minutes and then annealed by gradual cooling to room temperature in boiling water by removal of the heat source. Annealed DNAs were cloned into pGL4.17 vectors at BglII and BamHI sites.

To make pGL-Col10WT, pGL-Col10AM and pGL-Col10SM, the following minimal promoter with the sequence was inserted between BglII and HindIII of pGL4.17 backbone: ctagggggcggcccgcggtttgggccggtttgccagcctttggagcgaccgggagcatataactggagcctctgccgggggaaga. The Col10a1 enhancer sequences as shown were synthesized by Integrated DNA Technologies Inc. and inserted between KpnI and BglII.

For the construction of retroviral vectors, Fosl2, Jun, TAM67, and Sox9 cDNA were cloned into the pMX (Nosaka et al., 1999) vector backbone at BamHI and EcoRI sites. Viral constructs were transfected into plat-E cells (Morita et al., 2000) cultured in 10% fetal bovine serum (FBS)/ DMEM (Sigma-Aldrich, D5671) in order to produce viral particles.

Co-immunoprecipitation (Co-IP), SDS-PAGE and western blotting

Plasmids were transfected into HEK293T cells using FuGENE6 Transfection Reagent (Promega, E2691). Forty-eight hours post-transfection, nuclear extracts were prepared as previously described (Chew et al., 2005) with no dialysis step. The concentration of nuclear extract was determined on a Qubit Fluorometer (Life Technologies). Four-hundred microgram of extracts was used for one Co-IP reaction. After diluted five-fold (v/v) with ChIP lysis buffer (50 mM HEPES-KOH, pH 7.5, 140 mM NaCl, 1 mM EDTA, 10% Glycerol, 0.5% NP-40, and 0.25% Triton-X 100), the nuclear extracts were incubated overnight at 4 ºC with 25 μL of Dynabeads M-280 Sheep anti-mouse IgG (Life Technologies, 12201D), which was pre-coupled with 2.5μg anti-FLAG M2 antibodies (Sigma-Aldrich, F1804), in the presence of 0.38 U/μL Benzonase nuclease (Sigma-Aldrich, E1014). Beads were then washed three times with the RIPA buffer and boiled in 2x Laemmli buffer for 5 minutes.

Eluted materials and input samples were subjected to SDS-PAGE and blotted onto PVDF membranes. Immunostaining of the membranes was performed using peroxidase-conjugated anti-FLAG M2 antibodies (1:500; Sigma-Aldrich, A8592) or anti-Myc antibodies (1:1000; Abcam, ab9106). For the anti-Myc antibodies, HRP-conjugated goat anti-rabbit IgG was used for secondary antibodies (1:10000; Promega). Images were collected with ImageQuant LAS 4000mini (GE Healthcare UK Ltd.).

Mouse primary chondrocyte culture

P1 Swiss Webster mice (Jackson laboratory) or *Col10a1:mCherry* transgenic mice (Maye et al., 2011) were euthanized before rib dissection. Ribs were dissected under a standard dissection microscope to remove a segment containing the mitotic and hypertrophic chondrocyte regions while avoiding ossified regions. Superficial soft tissue was removed and rib segments were washed three times in Dulbecco's Phosphate Buffered Saline (DPBS) then digested with Collagenase D (2 mg/ml; Roche, 11088882001) for 40 minutes on a rotating rocker at 37 ºC rocking at 100 rpm. Following additional removal of soft tissue, ribs were collected into a fresh tube for an additional 3-hour digestion on a rocker at 37 ºC with several changes of digestion medium. Digested cells were filtered through a 40 μm filter and collected in

αMEM (Life Technologies, 12571071)/ 10% FBS with antibiotics and plated at ~95% confluence onto the desired culture plates.

SR11302 (R&D Systems, 2476) was dissolved in DMSO to generate a 100 mM stock concentration and kept at -70 ^{o}C. Stock solution was further diluted in α-MEM/10% FBS before applying to chondrocyte cultures. 1% ITS liquid media supplement (Sigma-Aldrich, I3146) and 20 mM Pi (sodium phosphate) were added to the medium to stimulate chondrocyte hypertrophy. Cells were cultured for two weeks with media changes every other day.

In gain-of-function analyses, isolated primary rib chondrocytes were transduced with viruses, and total RNA was harvested 3 days post-transduction with NucleoSpin RNA kit (Clontech, 740955) according to the manufacture's instruction. cDNAs were made with Superscript III reverse transcriptase (Life technologies, 18080-044). About 100 ng of cDNA was used for each quantitative PCR reaction using SYBR Green Master Mix with SYBR Premix Ex Taq II (Takara, RR820A) on ViiA 7 real-time PCR system (Applied Biosystems). The difference in Ct values (delta Ct) among each sample was calculated for fold change.

Immunostaining

To knockout *Sox9* from mouse prehypertrophic chondrocytes, we crossed Sp7-Cre (Rodda and McMahon, 2006) with Sox9 floxed mice (Akiyama et al., 2002). E16.5 embryos were obtained, and limbs were isolated by dissection. Tissues were fixed in 4% PFA/PBS for 1 hour at 4 °C and soaked in 30% sucrose/PBS overnight at 4 °C. After embedding in OCT compound, cryosections were generated at 8~10 μm. Sections were washed with PBS for 3 X 5 minutes and fixed again in 4% PFA for 20 minutes. Fixed sections were treated with 0.1 M Glycine/PBS for 25 minutes and washed with 0.1% Tween-20 /PBS (PBST) three times before blocking with 3% bovine serum albumin (Sigma-Aldrich, A7960) and 1% heat inactivated sheep serum (Sigma-Aldrich, S2263) in PBST for 30 minutes. The following antibodies where used in these studies: anti-Sox9 (1:500; Millipore, AB5535), anti-Sp7 (1:5000; Abcam, ab22552), anti-Col10a1 (1:1000; Cosmo Bio Co. LTD, LSL-LB-0092), anti-CD31 (1:1000; BD Pharmingen, 553370), and anti-Jun (1:1000; Abcam, ab31419), in combination with Alexa Fluor 488 (1:500; Life Technologies), Alexa Fluor 555 (1:500; Life Technologies) and Alexa Fluor 637 (1:500; Life Technologies). Primary antibodies were incubated overnight at 4 °C in blocking buffer at specified dilutions, followed by washing with PBST and incubation with secondary antibodies in blocking buffer for 1 hour at room temperature. Stained sections were mounted with Vectashield Mounting Medium containing DAPI (Vector laboratories, H-1200) before imaging. Images were captured with Zeiss Axio scanner (Carl Zeiss) by tiling high resolution images and processed with Zeiss Zen lite software (Carl Zeiss).

SUPPLEMENTARY REFERENCES

Akiyama, H., Chaboissier, M. C., Martin, J. F., Schedl, A. and de Crombrugghe, B. (2002). The transcription factor Sox9 has essential roles in successive steps of the chondrocyte differentiation pathway and is required for expression of Sox5 and Sox6. *Genes Dev* **16**, 2813-2828.

Bailey, T. L., Boden, M., Buske, F. A., Frith, M., Grant, C. E., Clementi, L., Ren, J., Li, W. W. and Noble, W. S. (2009). MEME SUITE: tools for motif discovery and searching. *Nucleic Acids Res* **37**, W202-208.

Chew, J. L., Loh, Y. H., Zhang, W., Chen, X., Tam, W. L., Yeap, L. S., Li, P., Ang, Y. S., Lim, B., Robson, P., et al. (2005). Reciprocal transcriptional regulation of Pou5f1 and Sox2 via the Oct4/Sox2 complex in embryonic stem cells. *Mol Cell Biol* **25**, 6031-6046.

Eberhart, J. K., He, X., Swartz, M. E., Yan, Y. L., Song, H., Boling, T. C., Kunerth, A. K., Walker, M. B., Kimmel, C. B. and Postlethwait, J. H. (2008). MicroRNA Mirn140 modulates Pdgf signaling during palatogenesis. *Nat Genet* **40**, 290-298.

Huang da, W., Sherman, B. T. and Lempicki, R. A. (2009). Systematic and integrative analysis of large gene lists using DAVID bioinformatics resources. *Nature protocols* **4**, 44-57.

Ji, H., Jiang, H., Ma, W., Johnson, D. S., Myers, R. M. and Wong, W. H. (2008). An integrated software system for analyzing ChIP-chip and ChIP-seq data. *Nat Biotechnol* **26**, 1293-1300.

Jiang, H., Wang, F., Dyer, N. P. and Wong, W. H. (2010). CisGenome Browser: a flexible tool for genomic data visualization. *Bioinformatics* **26**, 1781-1782.

Kan, A., Ikeda, T., Saito, T., Yano, F., Fukai, A., Hojo, H., Ogasawara, T., Ogata, N., Nakamura, K., Chung, U. I., et al. (2009). Screening of chondrogenic factors with a real-time fluorescence-monitoring cell line ATDC5-C2ER: identification of sorting nexin 19 as a novel factor. *Arthritis Rheum* **60**, 3314-3323.

Maye, P., Fu, Y., Butler, D. L., Chokalingam, K., Liu, Y., Floret, J., Stover, M. L., Wenstrup, R., Jiang, X., Gooch, C., et al. (2011). Generation and characterization of Col10a1-mcherry reporter mice. *Genesis* **49**, 410-418.

McLean, C. Y., Bristor, D., Hiller, M., Clarke, S. L., Schaar, B. T., Lowe, C. B., Wenger, A. M. and Bejerano, G. (2010). GREAT improves functional interpretation of cis-regulatory regions. *Nat Biotechnol* **28**, 495-501.

Morita, S., Kojima, T. and Kitamura, T. (2000). Plat-E: an efficient and stable system for transient packaging of retroviruses. *Gene Ther* **7**, 1063-1066.

Nosaka, T., Kawashima, T., Misawa, K., Ikuta, K., Mui, A. L. and Kitamura, T. (1999). STAT5 as a molecular regulator of proliferation, differentiation and apoptosis in hematopoietic cells. *EMBO J* **18**, 4754-4765.

Rodda, S. J. and McMahon, A. P. (2006). Distinct roles for Hedgehog and canonical Wnt signaling in specification, differentiation and maintenance of osteoblast progenitors. *Development* **133**, 3231-3244.

Vokes, S. A., Ji, H. K., McCuine, S., Tenzen, T., Giles, S., Zhong, S., Longabaugh, W. J. R., Davidson, E. H., Wong, W. H. and McMahon, A. P. (2007). Genomic characterization of Gli-activator targets in sonic hedgehog-mediated neural patterning. *Development* **134**, 1977-1989.

Zhang, X., Peterson, K. A., Liu, X. S., McMahon, A. P. and Ohba, S. (2013). Gene regulatory networks mediating canonical Wnt signal-directed control of pluripotency and differentiation in embryo stem cells. *Stem Cells* **31**, 2667-2679.

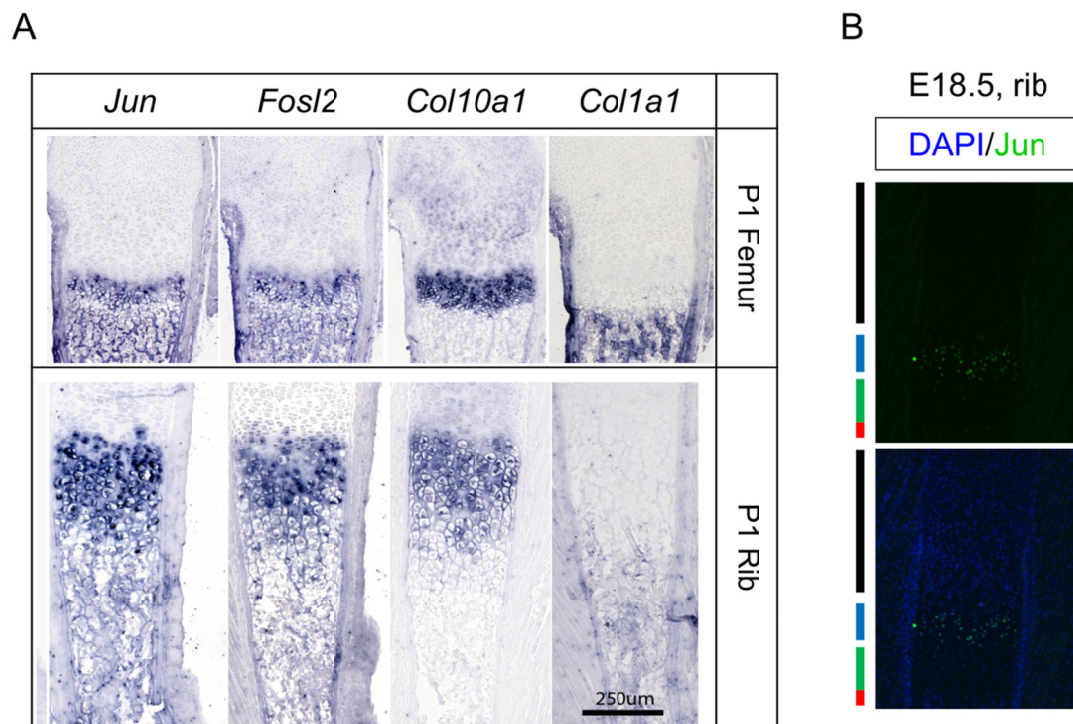**SUPPLEMENTARY FIGURES AND TABLES**

Figure S1. AP-1 expression in developing mouse rib and femur (Related to Figure 1, showing expressions of AP-1 and chondrocyte markers in tibia)

(A) *In situ* hybridization of *Jun*, *Fosl2*, *Col10a1*, and *Col1a1* on postnatal day 1 (P1) mouse rib and femur sections.

(B) Immunohistochemistry of Jun on E18.5 mouse rib sections stained with DAPI. See also Figure 1 for color bar code.

A

Row 1 (Sox9 Motif Enrichment):

All Sox9 Peaks (20862) (1.33, 29338/51454)
All Jun Peaks (99162) (1.07, 111696/215850)
Jun-Sox9 shared Peaks (16892) (1.28, 22803/40598)
Jun only Peaks (81862) (1.03, 88611/174431)

Sox9 Motif to Peak Center(nt)

Row 2 (AP-1 Motif Enrichment):

All Sox9 Peaks (20862) (1.89, 29609/45326)
All Jun Peaks (99162) (1.67, 112342/179705)
Jun-Sox9 shared Peaks (16892) (2.04, 26187/39013)
Jun only Peaks (81862) (1.58, 86155/140692)

AP-1 Motif to Peak Center(nt)

B

Jun only peaks
Jun only peak matched control regions
Jun-Sox9 shared peaks
Jun-Sox9 shared peak matched control regions
* p-value < 2.2e-16

Log10(Jun Reads counts)

C

GO Biological Process
Mouse Phenotype
MGI Expression

GO enrichment in Sox9 - Jun shared peaks

cartilage development
extracellular matrix organization
induction of apoptosis
induction of programmed cell death
chondrocyte differentiation
abnormal cartilage development
abnormal chondrocyte morphology
abnormal epiphyseal plate morphology
abnormal long bone epiphyseal plate morphology
abnormal long bone hypertrophic chondrocyte
TS24_limb
TS23_tibia
TS23_otic capsule
TS24_forelimb
TS21_embryo; skeleton

-log10(Binomial p value)

GO enrichment in Jun only peaks

extracellular matrix organization
homeostasis of number of cells
stem cell development
actin filament organization
chondrocyte differentiation
abnormal epiphyseal plate morphology
abnormal long bone epiphyseal plate morphology
abnormal long bone hypertrophic chondrocyte zone
abnormal chondrocyte morphology
disproportionate dwarf
TS24_limb
TS24_forelimb
TS21_embryo; skeleton
TS23_cricoid
TS20_rib pre-cartilage condensation

GO Biological Process
Mouse Phenotype
MGI Expression

-log10(Binomial p value)

Figure S2. Sox9 and AP-1 motif enrichment in Sox9 and Jun ChIP-seq peaks (Related to Figure 2, showing AP-1 and Sox9 motif enrichment in Sox9 and Jun shared peak regions as well as Jun only peak regions)

(A) Enrichment of Sox9 and AP-1 motifs in Sox9 and Jun ChIP-seq peaks. AP-1 and Sox9 motifs were mapped to Jun and Sox9 peaks as well as Jun-Sox9 shared peaks and Jun only peaks with expansion of peak size into 800 bp around peak center. Histograms show a centered enrichment of each motif with each peak. Numbers at top of each histogram displays the motif enrichment within the central 400 bp grey window versus total number of motifs in two distal 200 bp windows. Red: total number of peaks. Green: Motif count in central 400 bp grey window (from -200 bp to +200 bp) out of the total motif count in 800 bp window (from -400 bp to +400 bp). Blue: Motif enrichment measured by (total motif count from central 400 bp grey window)/ (total motif count from the -400 bp to -200 bp and +200 bp to +400 bp windows).

(B) Comparison of Jun ChIP-seq read counts between Jun-Sox9 shared peak regions and Jun-only peak regions. The read counts in matched control regions are also shown for each peak set. Jun-Sox9 shared peak regions show higher enrichment of Jun ChIP-seq read counts than Jun-only peak regions. Asterisk indicates statistical significance.

(C) GREAT GO analysis of Jun-Sox9 shared peak region and Jun only peak regions. Top 5 enriched GO terms of three categories are presented: Biological Processes (red), Mouse Phenotypes (Green) and MGI Expression (Blue).
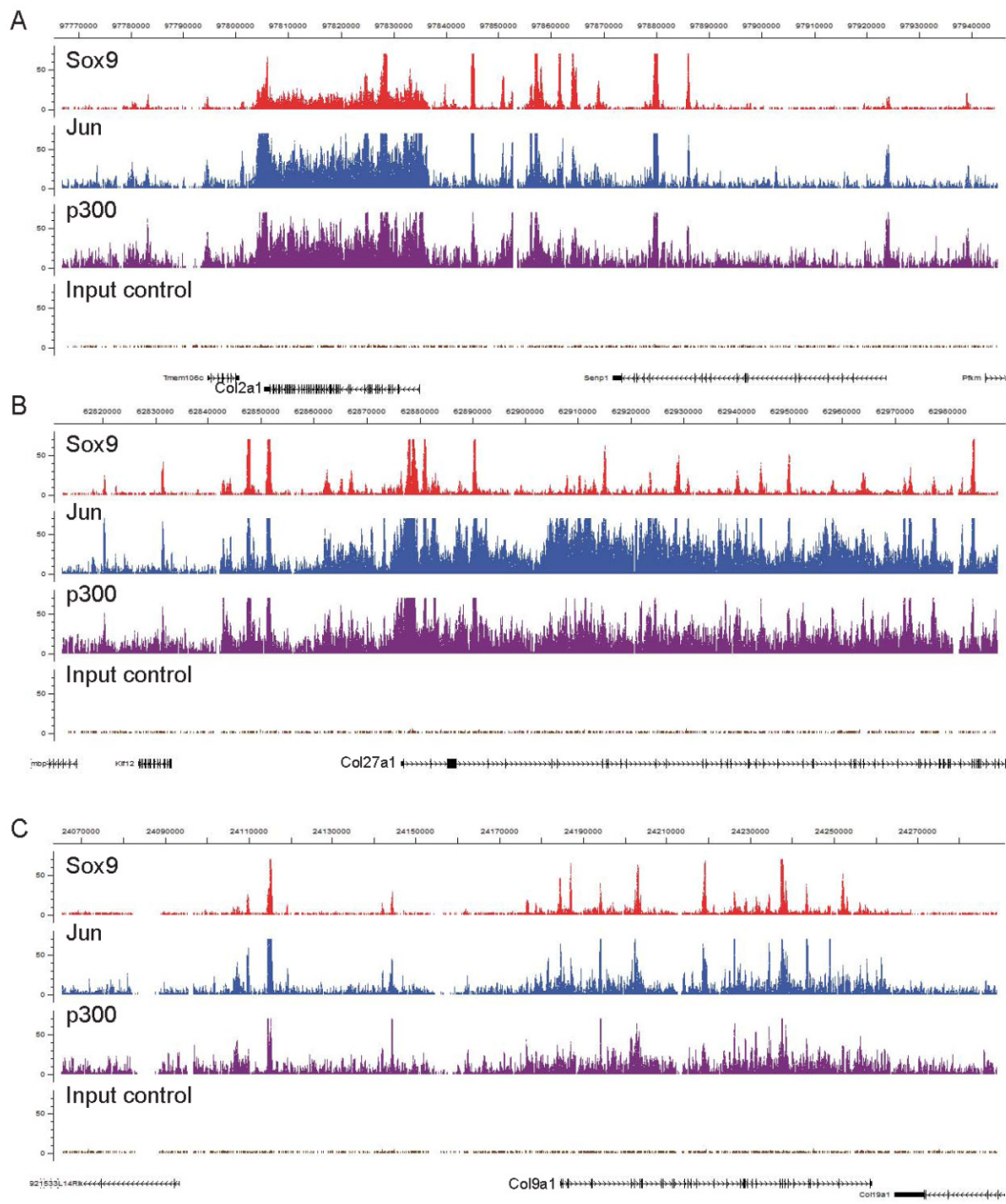
Figure S3. Sox9 and AP-1 binding clusters around chondrocyte-related genes (Related to Figure 2C, showing multiple interaction sites around genes encoding matrix proteins that are expressed at high levels in chondrocytes)

Screenshots for bindings of Sox9, Jun, and p300 around *Col2α1* gene (A), *Col27α1* gene (B), and *Col9α1* gene (C) are shown. Co-engagement of Sox9 and Jun, accompanied by p300, is observed at multiple sites.
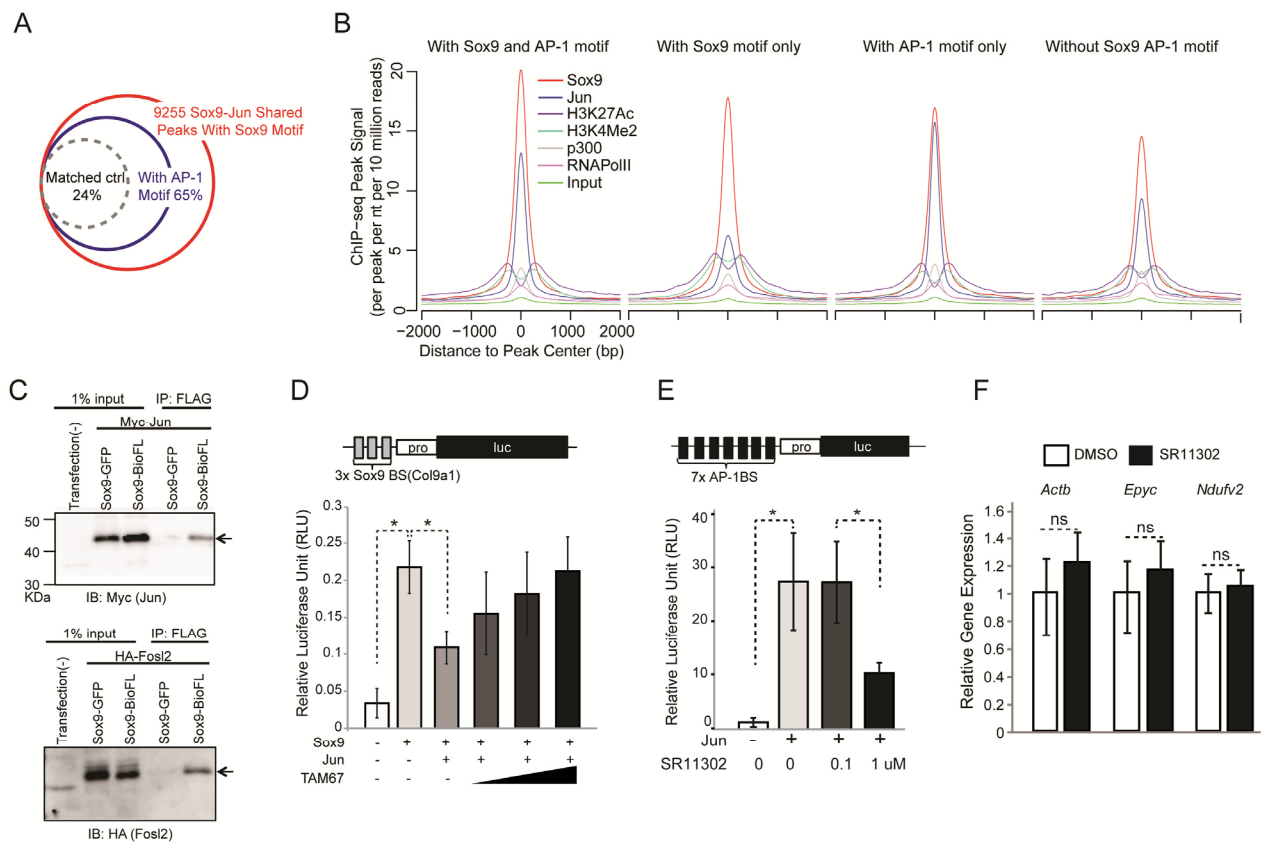
Figure S4. Possible interaction of Jun and Sox9 (A-C), effects of TAM67 on the Jun-Sox9 interaction (D), and effects of SR11302 on AP-1 activity and house-keeping function of cells (E and F) (Related to Figures 2-5, showing enrichment of AP-1 and Sox9 motifs, active enhancer histone marks in Jun-Sox9 shared peak regions, interaction between Sox9 and Jun/Fosl2, and verification of TAM67 and SR11302)

(A) Enrichment of both Sox9 and AP-1 binding motifs in Sox9-Jun shared peak regions. Compared to 24% in matched controls, 65% of Jun-Sox9 shared peak regions containing Sox9 motifs also contain AP-1 motifs.

(B) Relative enrichment of ChIP-seq signals of Sox9 (red), Jun (black), H3K27Ac (purple), H3K4Me2 (blue), p300 (grey), RNAPolII (violet) and Input (green) in category of peaks. X-axis indicates ChIP-seq signals plotted on a 4 kb window surroundings peak centers. Y-axis indicates normalized ChIP-seq signals.

(C) Physical association between Sox9 and Jun or Fosl2. HEK293T cells were co-transfected with Myc-tagged Jun (Myc-Jun) or HA-tagged Fosl2 (HA-Fosl2) with either GFP-fused Sox9 (Sox9-GFP) or Biotin-FLAG-tagged Sox9 (Sox9-BioFL). Immunoprecipitation was performed with FLAG tag, followed by immunoblot with Myc tag or HA tag. Data shows Sox9-BioFL, but not Sox9-GFP, can co-immunoprecipitate with Myc-Jun or HA-Fosl2.

(D) Interference of Jun-Sox9 interaction on enhancer activities of 3xSox9BS (Col9a1) by TAM67. In luciferase reporter assays, 3xSox9BS (Col9a1) reporter was activated with Sox9 but inhibited with Jun, and supplementation of TAM67 with increased concentration inhibited the effect of Jun on the Sox9-mediated activation of the reporter.

(E) Inhibition of AP-1 activity by SR11302. HEK293T cells were treated with SR11302 at different concentrations at 1 day after transfection of Jun and the 7xAP-1BS reporter construct. At 3 days post-transfection, cells were collected for relative luciferase expression assay. Jun activates luciferase reporter ($p < 0.001$). SR11302 inhibits this reporter activity at 1 µM compared to 0.1 µM ($p < 0.01$). Asterisks indicate statistical significance.

(F) No effect of SR11302 on endogenous housekeeping gene expression. mRNA expression of *Actb*, *Eypc* and *Ndufv2* were tested by RT-qPCR in chondrocytes treated with SR11302 showed no statistical significance (ns) from untreated controls.
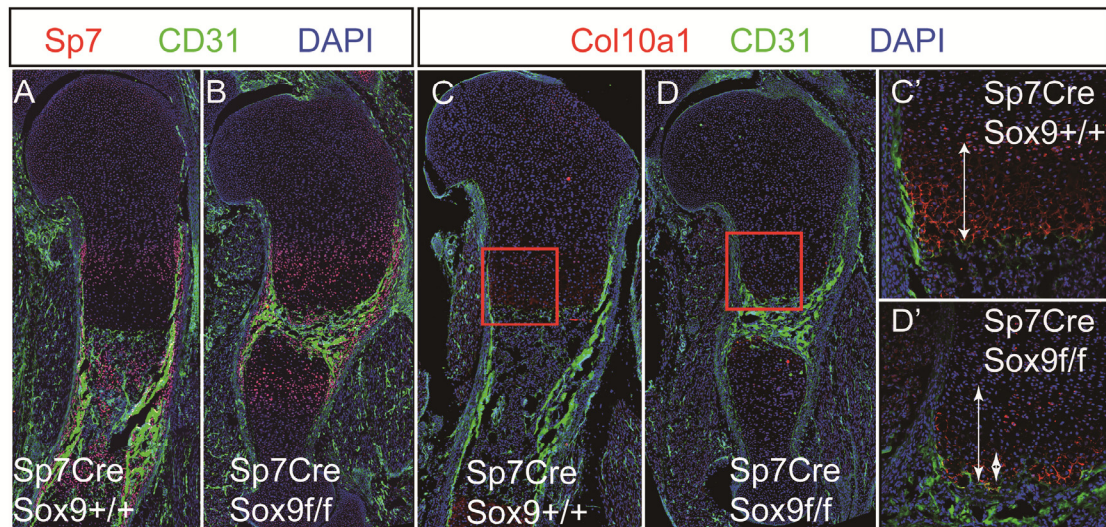
Figure S5. Loss of hypertrophic chondrocytes following Sox9 removal from prehypertrophic chondrocytes in the mouse humerus (Related to Figure 6, showing cooperative induction of *Col10a1* by Sox9 and AP-1). Sections from E16.5 Sp7Cre:*Sox9*f/f (experimental) or Sp7Cre:*Sox9*+/+ (control) mice were immunostained with Sp7 (red, prehypertrophic chondrocytes) (A and B) and Col10a1 (red, hypertrophic chondrocytes) (C and D), as well as CD31 (green, endothelial cells in vasculature) and DAPI (blue, nuclei staining) (A-D). Boxes in (C) and (D) highlight the Sp7 (prehypertrophic) and Col10a1 hypertrophic chondrocyte domains and are magnified in (C') and (D'), respectively.

```
Chimp   TTAATTAACGATCCACAGATGTGCAAATGAATAGGCAAGCTTAATAGTAGCTAACTGCCA
Mouse   GAAATCTTTGGGAAATGAATGAATGGATGACCCAGGGTACGTAATGGCAGCTAATTGCTA
Human   TTAATTAACGATCCACAGATGTACAAATGAATAGGCAAGCTTAATAGTAGCTAACTGCCA
         ***   *   *   ***   ****   *    * **** * ****** *** *

Chimp   GATGTGAAAAAAATCATTATTCATATTTGATATTTAAAAAAAATTACTCAGGTTATAGAGT
Mouse   CATGTGCAAAAC-CAGCGATTCATATTTGATATT--GAAAGCTCTTTGGGCTTACTGGCT  AP-1_M1
Human   GATGTGAAAAAAATCATTATTCATATTTGATATTTAAAAAAAATTACTCAGGTTATAGAGT
         ***** ****    **************** ***   *   * *** * *

Chimp   TTAAAGAGTATGGCTCTCTGTTTTGAGTGGAATGGGTTTCCTTCATAAAGCCACAGACTA
Mouse   TGAGAGGGTTGGGCCTCCTGTTTCACGTAGAATAAGC-TCCTTCATAAAGTCACAGACCA
Human   TTAAAGAGTATGGCTCTCTGTTTTGAGTGGAATGGGTTTCCTTCATAAAGCCACAGACTA  (Chambers et al. 2002) Unknown
         * * ** **   ***    ******    ** ****  * * *********** ******* *

Chimp   GTCACTTCAAACAGCTACAAGTAAACACCCAGAGTAAAAATAGTTTTAAATACACAATTG
Mouse   GTCAGGCTGAACAGCTCCGAGGAAACACCCAGAATAAAAATAGTTTAATACACACAATTA  Sox9_M1
Human   GTCACTTCAAACAGCTACAAGTAAACACCCAGAGTAAAAATAGTTTTAAATACACAATTG  (Leung et al. 2011) Sox9Motif
         ****   *******  *  **  *********** ************ * *  ********

Chimp   GGTG-GGGTGTGGCTAGAAAATATTCTGATTCTACAATCTGTTTTGGACAAGACAGTGCT
Mouse   GGTGTGGGTGTGGCCAGCAAATACTCTGATTCTACAATCTGTTTTGGACAGGGCAGTGCT  Sox9_M2
Human   GGTG-GGGTGTGGCTAGAAAATATTCTGATTCTACAATCTGTTTTGGACAAGACAGTGCT
         **** ********* **  ***** ****************************  * *******

Chimp   TCTTATGTGACTAACAAAGCAAACAGCAGTCAGATTCCTTGTGCTGAAATAAGTATACTA
Mouse   TCGTAGGTTGACTAACAAAGCAAACGGTAAACAGAGCCTGTATGCTGAAGTAAGGA-GTTA  AP-1_M6
Human   TCTTATGTGACTAACAAAGCAAACAGCAGTCAGATTCCTTGTGCTGAAATAAGTACACTA  (Gebhard et al. 2004) AP-1Motif
         ** **  ***************** *   *   ** ****   *  * ******* **** *   **

Chimp   TTTGCAAAAAGGGTTGAATGTCCAAGGCTTATTCAATAAGGACACCACATTTTCCAAAAC
Mouse   TTTGCCAAAAGGGCTGAATATCCA--GTCTGCT-AGTAAG-ACATCATGCTTCCCAAAGC
Human   TTTGCAAAAAGGGTTGAATGTCCAAGGCTTATTCAATAAGGACACCACATTTTCCAAAAC
         ***** *******   *****  ****   *   *   * * ****  ***  **  ** ***** *

Chimp   TAAAGGGGAGTATAGAATGACAAATACCCACATATATTTACATATCCCTAAAAGAAGACA
Mouse   TCGAG---AATATTGACTGAGATATGAACAT-TATTTAATCATATCCTCCAAAGAAGGCA  AP-1_M7
Human   TAAAGGGGAGTATAGAATGACAAATACCCACATATATTTACATATCCCTAAAAGAAGACA
         *   **    * *** ** *** * **    ** *** *    ******   ******* **
```

Chimp: chr6:117,257,227-117,257,705 (CSAC 2.1.4/panTro4). Mouse: chr10:34,105,362-34,105,828
(NCBI37/mm9). Human: chr6:116,449,273-116,449,751 (GRCh37/hg19)

Red: AP-1 motif; Green: Sox9 motif; *Italic bold*: essential nucleotide mutated; <u>Underlined</u>: previously verified sites.

Figure S6. Sox9 and AP-1 binding sites in a *Col10a1* enhancer region (Related to Figure 6, showing detailed Sox9 and AP-1 motif prediction in *Col10a1* enhancer)
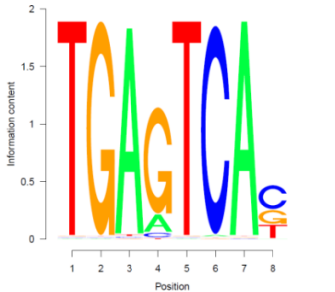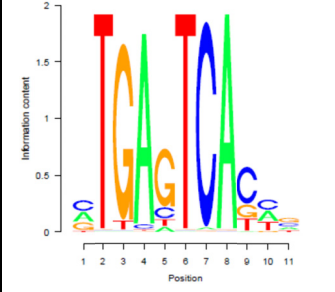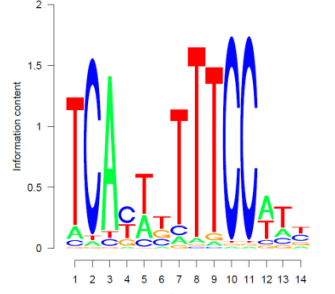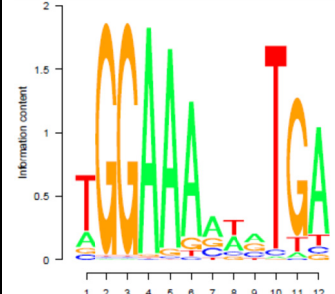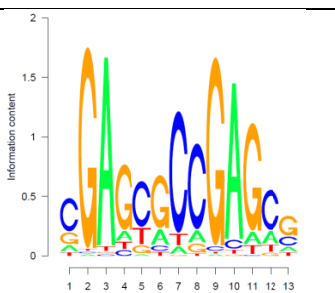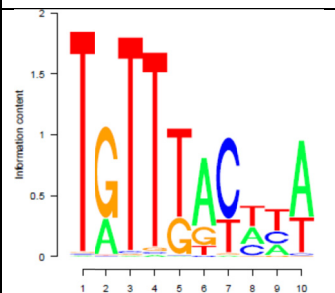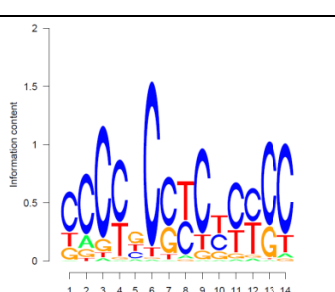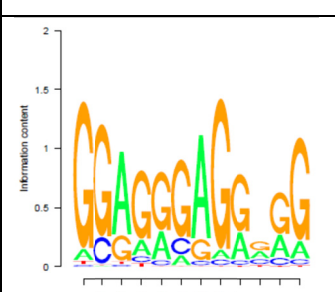
A published Col10a1 enhancer identified through ChIP-seq analyses contains multiple Sox9 and AP-1 motifs. The mouse *Col10a1* enhancer region (chr10:34,105,362-34,105,828; NCBI37/mm9) was blast searched for human and chimp orthologs, and aligned for nucleotide similarity. AP-1 motifs and Sox9 motifs predicted with Cisgenome package are marked by red and green, respectively. AP-1 motif AP-1_M6 and Sox9 motif Sox9_M2 match with ones reported in previous publications (Gebhard et al. 2004; Leung et al. 2011). Nucleotide mutations to either AP-1 binding sites or Sox9 binding sites were labeled as italic letters.
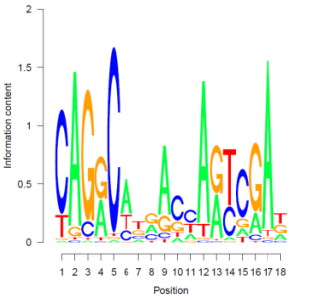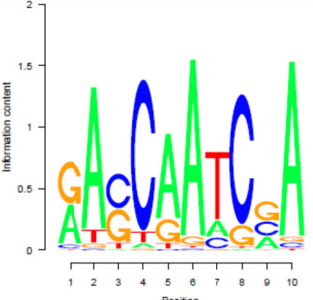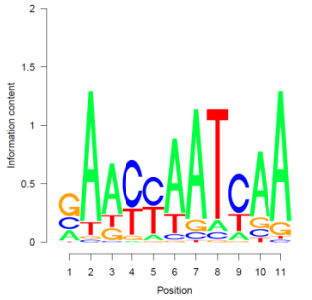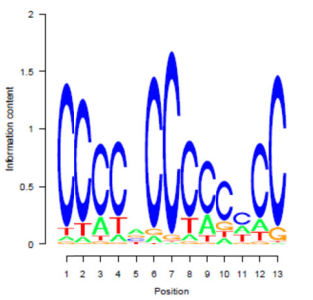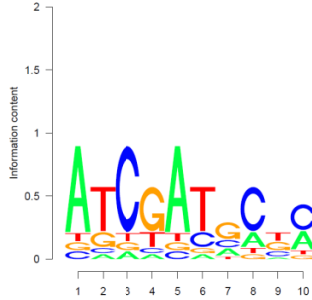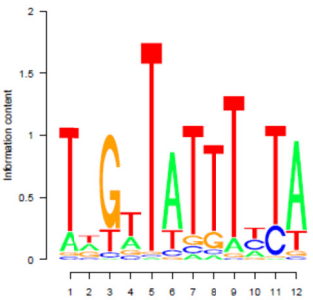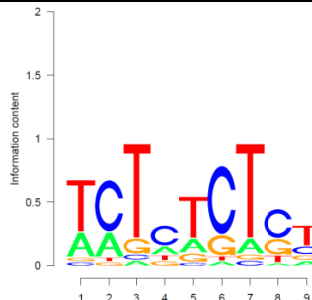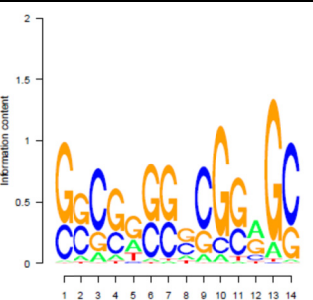
Table S1. Expression of AP-1 family members as well as skeletal markers in whole rib chondrocyte as well as *Col10a1:mCherry* sorted rib chondrocytes, determined by RNA-seq (Related to Figure 1, showing expressions of AP-1 and chondrocyte markers in tibia)
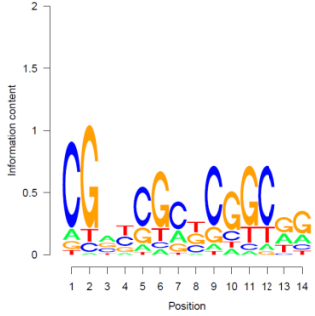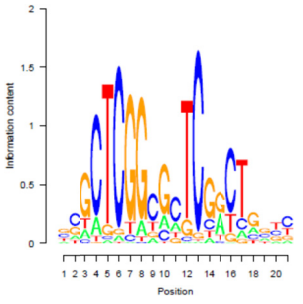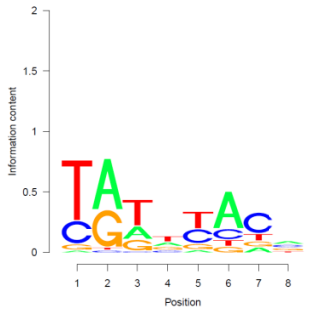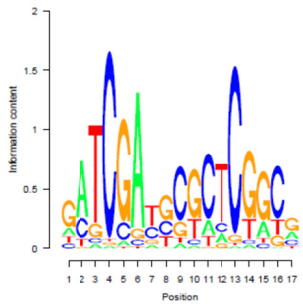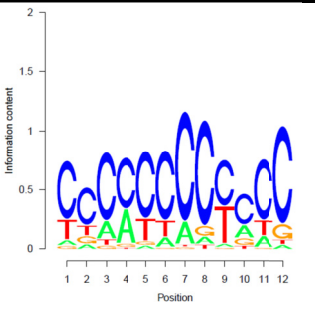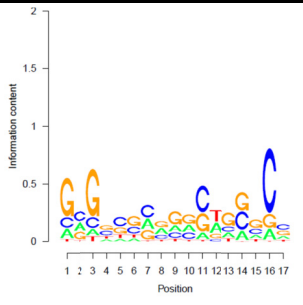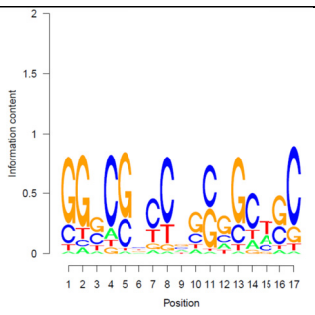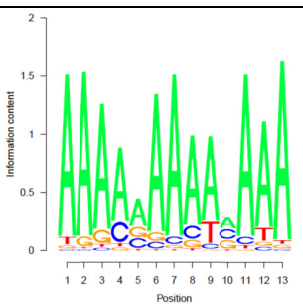
Gene	Refseq	Whole Rib	Col10a1:mCherry Sorted
Sox9	NM_011448	129.888*	91.503
Ucma	NM_001113558	778.062	82.0786
Col2a1	NM_001113515	16888	17408.4
Mef2c	NM_001170537	1.84271	20.7768
Ihh	NM_010544	2.99862	84.2572
Sp7	NM_130458	1.33544	31.1955
Nkx3-2	NM_007524	0.778057	5.82514
Pth1r	NM_001083936	14.4721	275.651
Col10a1	NM_009925	26.4948	5643.12
Ibsp	NM_008318	1.21598	49.6506
Mmp13	NM_008607	0.350414	148.554
Jun	NM_010591	157.053	56.8872
Junb	NM_008416	148.403	115.091
Jund	NM_010592	84.7652	41.9016
Fos	NM_010234	292.614	48.0042
Fosb	NM_008036	287.451	1.03116
Fosl1	NM_010235	0.649246	1.59364
Fosl2	NM_008037	23.471	21.3539
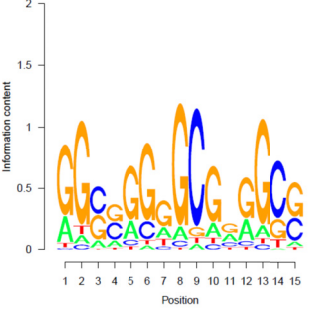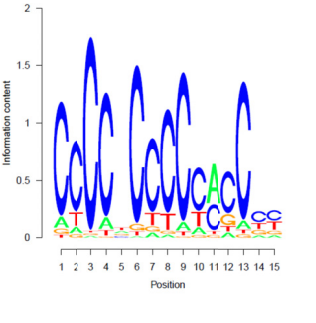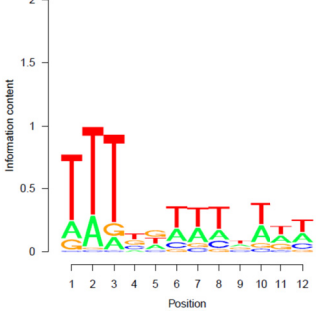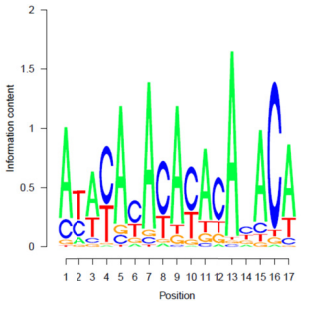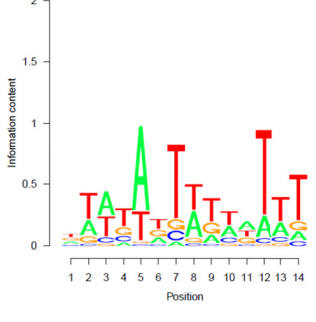
* RPKM value

Table S2. Top 10 motifs recovered from top 500 and 2000 Jun ChIP-seq peaks examining +/- 50bp around the computed peak center and matched control regions utilizing Cisgenome (Related to Figure 2, showing Cisgenome motif prediction verifying MEME motif prediction)

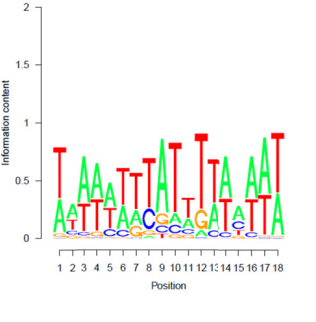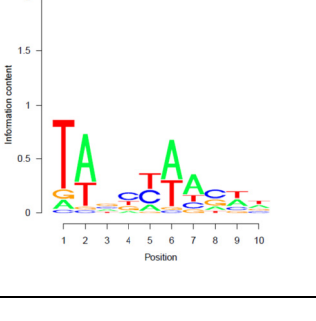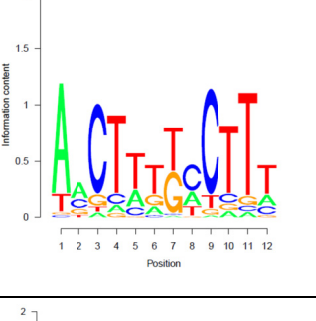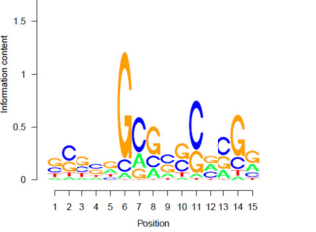| Data	Motif ranking	Top 500 peaks			Top 2000 peaks		
		seqLogo	Recovery Score	Matched Factors	seqLogo	Recovery Score	Matched Factors
Jun ChIP-seq dataset	1		6.205965	BACH1 BACH2 AP1 FRA1 AP1 AP1 NRF2 AP1 AP1 NFE2		6.103235	AP1_C FRA1 AP1_Q6 AP1 AP1_Q4 AP1_Q2 BACH2 NFE2
	2		2.924970	NFAT3 NFAT2 NFAT1 NFAT NFAT HELIOSA STAT5A STAT6 PARP STAT6		4.492112	NFAT3 NFAT2 NFAT NFAT1 NFAT_Q4 HELIOSA STAT5B STAT5A STAT1
	3		2.636923	DEAF1 HOXA13 KLF15 ZF5 HSF1 ZIC2 HOXC13 HIC1 STAT5A NRSE		4.085127	HNF3 FREAC4 HNF3B HNF3AL PHA HNF3A HNF3 FOXO3 FOX FOXP3
	4		2.219678	SP1 SP1SP3 PR PAX4 OBOX3 SP1 OTX1 SP1 DOBOX5 AR		3.251418	IK LYF1 TFIII PAX4 FPM315 SP3 MAZ PUR1 GATA4

5		2.113371	SMAD FOXP3 PAX AML NFY HP1SITE FACTOR TR4 LMAF P53 CP2		3.055590	CDPCR1 DUXL NKX52 HMX1 HMX3 BARHL2 CDPCR3 HD CDP MSX3
6		1.800168	DUXL MSX3 EN1 BARHL1 BARHL2 HOXB13 ALX3 NCX LIM1 K2B		2.977624	SP1_Q2 SP1_Q4 SP1_Q6 UF1H3B ETA SP1 KROX SP1_Q6 ZFP281 GKLF
7		1.619753	CDPCR1 CDP CDPCR3 HD MSX2 CART1 HOMEZ CDP OBOX2 POU6F1 POU6F1		2.767058	AMEF2 PAX4 MEF2 HMGIY HMEF2 HOXC13 HOXD10 ANTP HOXA9
8		1.638866	ATF DOBOX4 SOX9 SMAD AR PR OBOX2 TGIF AHR TAL1		2.454217	KROX HIC1 SREBP2 ZFX TGIF NANOG PUR1 CNOT3 HMX1

	9		1.495911	HIC1 E2F1 CREB STAF AP2 SZF11 GLI1 NFMUE1 PAX4 COUPTF		2.165546	ZIC2 ZF5 ZIC1 GLI3_02 GLI2 HIC1 HMX1 MSX2 CMYB
	10		1.047425	LHX9 HOXD8 PIT1 HFH8 PAX6 MSX1 TEF NURR1 HNF3 ICSBP		2.092176	CDPCR1 HSF2 CDP HSF1 CDPCR3 HD CDP HOMEZ PAX4 TCF4
Matched control regions	1		2.220248	ZNF219 PAX4 PR SP1SP3 PR ZIC2 ZIC1 WT1 MZF1		3.932972	HIC1_03 TATA NFY ATF AP2ALP HA AP2 LMO2CO M LHX9 HIC1 ZFX
	2		1.233748	HIC1 CTCF HOXA9 DEAF1 GLI3 AP2 MTF1 GLI2 ZFX		3.397854	TCF3 FOXP1 FAC1 NANOG SMAD1 ANTP STAT4 PAX4 IRF3 HNF3B

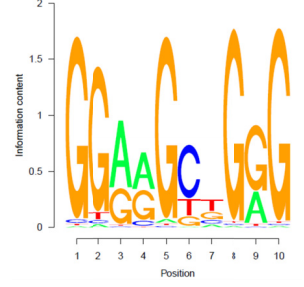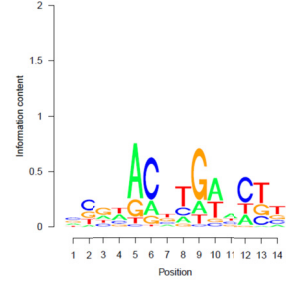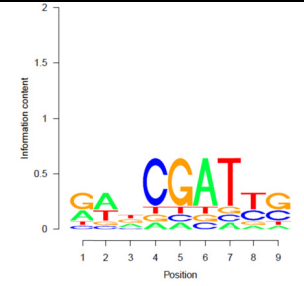| 3 | | 1.905892 | SP1
SP1
SP1
AP2
KROX
ZF5
PAX5
DEAF1
TATA | | 2.870400 | ZFP281
UF1H3B
ETA
SP1
SP1
SP4
SP1
KROX
SP1
KLF15 |
4		1.011503	HOMEZ IRF3 DMRT4 PU1 GATA3 YY1 BARHL2 SRY PAX4		2.204697	PBX1 PIT1 IRX2 AREB6 IRXB3 IRX5 PEA3 OCT1 FAC1 MYCMAX
5		1.101541	DBX1 HOXA9 HOXA10 HOXD10 OCT2 PBX1 POU2F3 HOXD13 CDX1		2.069564	DBX1 NCX HOXA10 BCL6 IRX5 IRXB3 HOXA9 IRX4 DBX2 HOXA13
6		0.669284	OCT1 IRX3 IRX4 IRX5 IRX2 HOXA2 NCX VAX1		1.853307	PXRRXR TCF4 SOX4 PXRRXR DR1 HNF1B NKX21 SRF OBOX3 OBOX1
7	No logo	0.207511	NKX52 OBOX6 HMX3 HOXD12 VAX1 HOXB9 SREBP2 HOXB13 CMYB		1.515860	HIC1 E47 TATA ARNT ARNT MYOD PAX4 PITX3 ERR2

8	No logo	0.000220	ELK1 STAT1 PITX2 LH2 AR SRF PBX1 NFY TST1		1.032602	VDR EGR KLF15 LYF1 OLF1 TAL1 SP1 TFIIA PTF1BETA ZFP281
9	No logo	0.000220	ELK1 STAT1 PITX2 LH2 AR SRF PBX1 NFY TST1		0.691074	NFY_Q6 PXRRXR PAX3_B PXRRXR MYOD TAL1 NKX23 NANOG NKX22 PU1
10	No logo	0.000220	ELK1 STAT1 PITX2 LH2 AR SRF PBX1 NFY TST1		0.491009	HOMEZ CDP NKX52 HMX3 HOXA4 CART1 ALX4 NKX29 SRF PKNOX2

Table S3. Top 10 motifs recovered from top 500 Jun only ChIP-seq peaks examining +/-50bp around the computed peak center utilizing Cisgenome (Related to Figure 2, showing Cisgenome motif prediction that Sox9 motif is not enriched in Jun only regions)

Motif ranking	seqLogo	Recovery Score	Matched Factors
1		4.985652	M00174_AP1 M00490_BACH2 M00199_AP1 M00517_AP1 M01267_FRA1 M00188_AP1 M00173_AP1 M00926_AP1 M00925_AP1 M00172_AP1FJ
2		4.665098	M00037_NFE2 M00199_AP1 M00925_AP1 M00517_AP1 M00926_AP1 M00284_TCF11MAFG M00174_AP1 M01267_FRA1 M00924_AP1 M00821_NRF2
3		3.062235	M00302_NFAT M01734_NFAT3 M01718_NFAT2 M00935_NFAT M01281_NFAT1 M01004_HELIOSA M00494_STAT6 M00493_STAT5A M01212_STAT1STAT1 M01207_ETS2
4		2.559199	M00983_MAF M01267_FRA1 M00199_AP1 M00926_AP1 M00188_AP1 M00517_AP1 M00174_AP1 M00925_AP1 M00172_AP1FJ M00821_NRF2

5		1.851585	M01122_ZNF219 M00982_KROX M00931_SP1 M01273_SP4 M00933_SP1 M01303_SP1 M01343_PITX3 M00957_PR M00954_PR M01364_OBOX2
6		1.374859	M01390_DUXL M01357_PBX1 M01478_CPHX M00517_AP1 M00037_NFE2 M00924_AP1 M01391_PAX6 M01324_OCTAMER M00174_AP1 M00926_AP1
7		1.063022	M01308_SOX4 M01014_SOX M01332_BARHL1 M01446_BARHL2 M00983_MAF M01341_MSX3 M01340_BARX1 M01153_PXRRXR M01315_NKX52 M01152_PXRRXR
8		0.986061	M01483_DBX1 M01420_NCX M01357_PBX1 M01328_ISL2 M01432_HOXD8 M01413_HMX3 M01315_NKX52 M01472_IRX5 M01399_HB24 M00999_AIRE

| 9 | | 0.624240 | M01355_ALX3
M01487_HOXA1
M01354_OCT1
M01012_HNF3
M01405_IRX2
M01452_HOX13
M01391_PAX6
M01385_PAX4
M01420_NCX
M01472_IRX5 |
| 10 | | 0.553769 | M00929_MYOD
M00539_ARNT
M01072_HIC1
M01073_HIC1
M00004_CMYB
M01489_NKX61
M01370_HOXA4
M01036_COUPTF
M01424_HOXB4
M00469_AP2ALPHA |